

Evidence for a retinal velocity memory underlying the direction of anticipatory smooth pursuit eye movements

T. Scott Murdison,^{1,2} Chanel A. Paré-Bingley,^{1,2} and Gunnar Blohm^{1,2}

¹Centre for Neuroscience Studies, Queen's University, Kingston, Ontario, Canada; and ²Canadian Action and Perception Network (CAPnet), Toronto, Ontario, Canada

Submitted 13 November 2012; accepted in final form 13 May 2013

Murdison TS, Paré-Bingley CA, Blohm G. Evidence for a retinal velocity memory underlying the direction of anticipatory smooth pursuit eye movements. *J Neurophysiol* 110: 732–747, 2013. First published May 15, 2013; doi:10.1152/jn.00991.2012.—To compute spatially correct smooth pursuit eye movements, the brain uses both retinal motion and extraretinal signals about the eyes and head in space (Blohm and Lefèvre 2010). However, when smooth eye movements rely solely on memorized target velocity, such as during anticipatory pursuit, it is unknown if this velocity memory also accounts for extraretinal information, such as head roll and ocular torsion. To answer this question, we used a novel behavioral updating paradigm in which participants pursued a repetitive, spatially constant fixation-gap-ramp stimulus in series of five trials. During the first four trials, participants' heads were rolled toward one shoulder, inducing ocular counterroll (OCR). With each repetition, participants increased their anticipatory pursuit gain, indicating a robust encoding of velocity memory. On the fifth trial, they rolled their heads to the opposite shoulder before pursuit, also inducing changes in ocular torsion. Consequently, for spatially accurate anticipatory pursuit, the velocity memory had to be updated across changes in head roll and ocular torsion. We tested how the velocity memory accounted for head roll and OCR by observing the effects of changes to these signals on anticipatory trajectories of the memory decoding (fifth) trials. We found that anticipatory pursuit was updated for changes in head roll; however, we observed no evidence of compensation for OCR, representing the absence of ocular torsion signals within the velocity memory. This indicated that the directional component of the memory must be coded retinally and updated to account for changes in head roll, but not OCR.

anticipatory pursuit; velocity memory; head roll; ocular counterroll; reference frames; updating paradigm

THE HUMAN VISUOMOTOR SYSTEM constantly generates eye movements, such as saccades and smooth pursuit to foveate objects of interest, enabling us to selectively view moving objects with high acuity. While much research has investigated how retinal signals are used to drive these movements (e.g., Johnston and Everling 2008; Krauzlis 2004), there has been less focus on the role memorized signals play, such as those used for anticipatory pursuit movements. To counteract processing delays associated with visually guided pursuit, the brain can use a velocity memory encoded during preceding target exposures to accelerate the eyes prior to receiving any retinal input (e.g., Barnes 2008; Orban de Xivry and Lefèvre 2007), but how this memory is encoded and ultimately transformed into an anticipatory pursuit command remains largely unknown.

Address for reprint requests and other correspondence: G. Blohm, Centre for Neuroscience Studies, Queen's Univ., Botterell Hall, Rm. 229, 18 Stuart St., Kingston, Ontario, Canada K7L 3N6 (e-mail: gunnar.blohm@queensu.ca).

For visually guided smooth pursuit, it has been established that the retinal target velocity (retinal slip) is the primary driving signal for movement initiation (e.g., Ilg 2008; Ilg and Thier 2008; Krauzlis 2004; Lisberger 2010; Orban de Xivry and Lefèvre 2007). However, because the relative orientations of the eyes and the head change with head-on-shoulder and eye-in-head rotations, it is often the case that the retinal target direction is not spatially equivalent to the eye-in-head movement direction required to minimize that retinal slip; i.e., the retinal velocity vector must be rotated in some way to match the required motor output vector (Blohm and Lefèvre 2010). For example, during head roll toward the right shoulder, the eyes counterrotate about the gaze direction by a small angle (ocular torsion) toward the left shoulder in a phenomenon known as ocular counterroll (OCR). OCR is depicted in Fig. 1A, which shows the relative alignments of the head-centered (blue dashed lines), retinal (green dashed lines), and spatial (black dashed lines) axes under these conditions. As a result, retinal slip is rotated by the angle of OCR, while the required eye-in-head direction is rotated by the amount of head roll. Therefore, to produce spatially accurate pursuit, integration of retinal and both eye and head orientation signals in a geometrically correct, three-dimensional (3D) transformation is required (Blohm and Lefèvre 2010). The geometrical requirement for a 3D transformation of retinal slip signals can also arise during horizontal, vertical, or oblique gaze positions, during horizontal cyclovergence or cyclovergence, and during head movement-induced compensatory vestibulo-ocular reflex (VOR) movements, including OCR (Blohm and Lefèvre 2010). Blohm and Lefèvre (2010) observed spatially accurate visually guided pursuit during OCR and from vertical, horizontal, and oblique gaze positions. This led them to propose that two-dimensional (2D) retinal slip signals undergo a 3D visuomotor velocity transformation under each condition, meaning that the pursuit system uses extraretinal information about eye and head orientations to account for misalignments between the retinal target motion and the required head-centered motor output (Blohm and Lefèvre 2010). Here we investigated if the same type of spatially correct transformation exists within the anticipatory pursuit circuitry by determining the reference frame of the velocity memory underlying the direction of anticipatory pursuit.

Memory-driven anticipatory pursuit can be experimentally elicited and analyzed behaviorally (Barnes and Asselman 1991; Barnes et al. 1997, 2000; Barnes and Donelan 1999; Becker and Fuchs 1985; Blohm et al. 2003a, 2003b; Collins and Barnes 2005; Heinen et al. 2005; Knox 1996, 1998; Wells and Barnes 1998). In the present study, participants encoded a

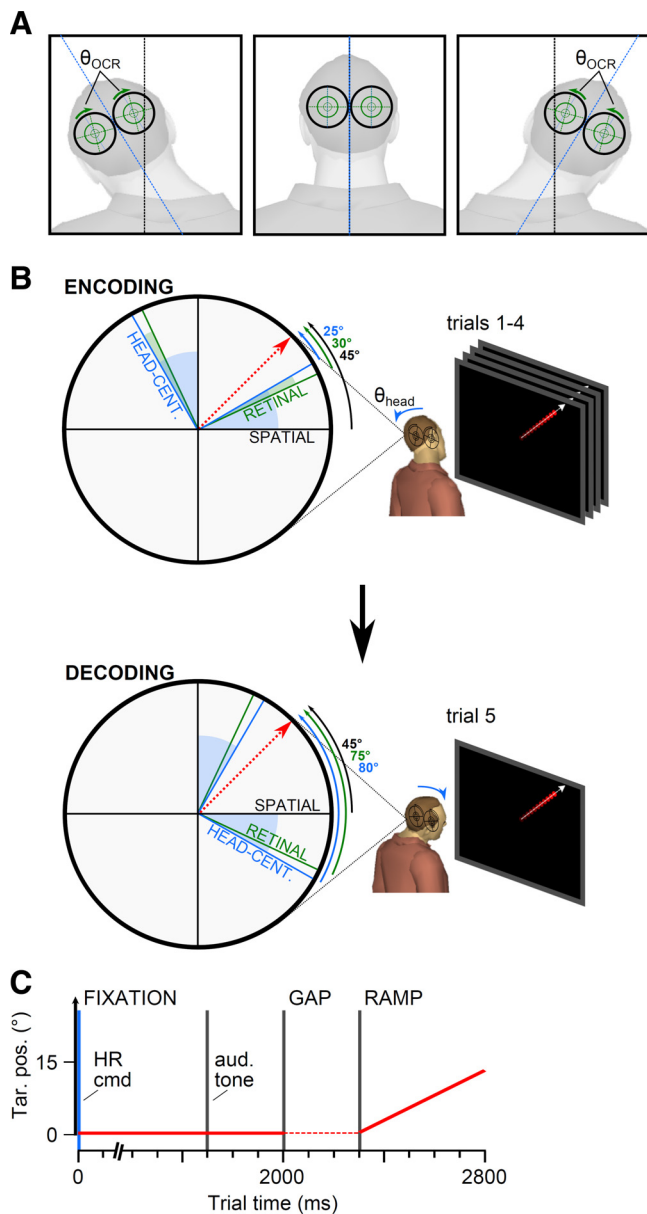


Fig. 1. Experimental rationale and setup. *A*: the eyes counterrotate [ocular counterroll (OCR)] during static head roll (HR), creating a misalignment between retinal (green), head-centered (blue), and spatial (black) axes. θ_{OCR} , OCR direction. *B*: the misalignment between retinal input and head-centered output exists both during encoding of the retinal velocity memory and during decoding of this memory. For a spatially correct transformation, not only must this memory use extraretinal eye and head position signals to account for these misalignments at encoding, but also across HR change prior to decoding. Note that, for an arbitrary HR, the spatial target direction (black text) remains constant, while the head-centered target direction (blue text) and the retinal target direction (green text) are misaligned and change with HR and encoding OCR. The shaded regions of these plots represent the signals across which velocity memory must be updated for spatially accurate anticipatory pursuit. θ_{head} , HR direction. *C*: trial time course. Participants performed each trial in three stages: fixation (2,000 ms), gap (300 ms), and ramp (500 ms). During the target ramp, participants pursued the target. At the start of each trial sequence, there was a verbal HR instruction (blue vertical), indicating to the participant the shoulder toward which the head should be rolled. Additionally, there were auditory tones (black verticals) 300 ms prior to target onset, at target onset, and 300 ms after target onset to improve anticipation gains (Barnes and Donelan 1999). Tar. pos., target position; HR cmd, HR command.

velocity memory used to drive anticipatory pursuit with their heads rolled toward one shoulder (inducing OCR), then used that velocity memory to drive anticipatory pursuit after rolling their heads toward the opposite shoulder. Using a reference frame point of view, we developed theoretical scenarios in which head and eye signals were or were not integrated into the velocity memory at encoding and/or updated prior to decoding. For example, if the velocity memory were coded in a retinal reference frame, only the 2D target trajectory information would be accounted for by the memory, and, to produce spatially accurate anticipatory pursuit after a head roll change, the memory would have to be updated across both head roll and OCR. Thus, by correlating directional anticipatory pursuit errors on memory decoding trials (after the head roll change) with different signals that should be present/absent in different coding schemes, we arrived at three working hypotheses: 1) the velocity memory would not be updated across eye and possibly head orientation changes, showing errors correlated at least with OCR and possibly also with head roll (retinal hypothesis); 2) the velocity memory would be updated across eye orientation changes but not head orientation changes, showing errors correlated with only head roll change (head-centered hypothesis); 3) the velocity memory would be completely updated across both eye and head orientation changes, and no systematic errors would occur on decoding trial anticipatory pursuit (spatial hypothesis).

We report that the velocity memory for anticipatory pursuit is updated across head roll changes, but does not compensate for OCR on encoding trials, satisfying the retinal hypothesis. This indicates that the directional component of the velocity memory does not include any torsional eye-in-head orientation information and must, therefore, be encoded in a retinal reference frame and is updated across head roll. We discuss the implications of this study for other memory- and nonmemory-based visuomotor experiments and make predictions about the neurophysiology underlying anticipatory pursuit.

METHODS

Hypotheses

We elicited memory-driven anticipatory pursuit of a predictable ramp stimulus. We then introduced a change in head roll between the encoding of this memory and its decoding to a motor command to observe the updating of this memory across head and eye orientation changes. Our updating paradigm allowed us to determine the reference frame of velocity memory encoding and decoding by dissociating the effects of head roll and ocular torsion signals at each stage. Figure 1*B* illustrates the potential rotational influences of each of these signals (circular plots: encoding and decoding head roll signals represented by blue shaded regions and encoding ocular torsion signal represented by green regions) on a theoretical pursuit target moving in the 45° direction on the screen. Depending on in which coordinate frames the velocity memory was encoded and decoded, the target direction, and therefore the anticipatory eye direction, would be rotated by varying amounts as a result of head roll and OCR. For example, if the participant rolls his head by 20° in the counterclockwise (CCW) direction during encoding trials (Fig. 1*B*, top), this rotates the head-centered axes by that amount relative to the spatial axes (blue in circular plot). In this arbitrary example, the OCR induced by head roll is 5° in the clockwise (CW) direction, meaning that the eyes (and thus the retinal axes) are only rotated by 15° CCW relative to the spatial axes. Thus the target direction in space, that

relative to head-centered axes and that relative to retinal axes, is not equivalent. Figure 1B shows this misalignment of target direction in different reference frames due to head roll and OCR in the encoding circular plot (*top*) with target directions of 45° in space (black text), 25° relative to the head (blue text), and 30° on the retina (green text). A change in head roll (and OCR) prior to the decoding trial (Fig. 1B, *bottom*) induces further misalignments in target direction relative to each set of axes, with the target still moving in the 45° direction in space, but in the 80° direction relative to the head and in the 75° direction on the retina. As such, the velocity memory should ideally account for the extraretinal head roll and OCR signals giving rise to these geometrical misalignments at memory encoding and must be updated prior to decoding for spatially accurate anticipatory pursuit.

Barnes and Collins (2008) observed similarities between preceding visually guided pursuit and the current anticipatory response, leading to the hypothesis that this velocity memory is based on the eye velocity (EV) of preceding visually guided pursuit. As the extraocular muscles generating this velocity are head-fixed, this suggests that velocity memory for anticipatory pursuit exists in a head-centered reference frame. In this case, the directions of anticipatory trajectories would be spatially accurate across changes in gaze location, but would have to be updated across changes in head orientation to be spatially accurate.

In contrast, recent evidence has shown that information about head rotations and the resulting VOR movements is used in predictive pursuit during transient target disappearance (Ackerley and Barnes 2011). Additionally, the pursuit system is known to share its eye-in-head position and velocity information with the saccadic system (Blohm et al. 2003a, 2005, 2006; de Brouwer et al. 2001, 2002a, 2002b; Gellman and Carl 1991; Keller et al. 1996; Keller and Johnsen 1990; Orban de Xivry et al. 2006; Ron et al. 1989a, 1989b), suggesting that these signals could also be accessible to the anticipatory pursuit system to be encoded in velocity memory. Therefore, the anticipatory pursuit system could have access to all of the extraretinal signals required for a 3D visuomotor transformation of velocity memory, meaning that a velocity memory could be coded in a spatial frame rather than a head-centered frame and so requires no updating across any extraretinal changes to produce spatially accurate anticipatory pursuit.

Another hypothesis about the reference frame in which the velocity memory for anticipatory pursuit is encoded comes from experiments investigating position memory during visuospatial memory tasks (Fiehler et al. 2010; Henriques et al. 1998). These experimenters found that both for saccades and for reaches, memorized targets are coded in retinal frames, meaning that target location information needs to be updated across changes of gaze locations, as well as head orientations to be spatially accurate (Fiehler et al. 2010; Henriques et al. 1998). In this study, we ask whether velocity memory is coded in 1) a retinal reference frame (requiring updating across eye orientation and head orientation changes); 2) a head-centered reference frame (requiring updating across only head orientation changes); or 3) a spatial reference frame (requiring no updating).

Participants

Seven human participants (aged 20–36 yr, five men) were recruited after informed consent was obtained. Five of those seven participants were naive as to the purpose of the experiment. All participants had normal or corrected-to-normal vision and did not have any known neurological, oculomotor, or visual disorders. All procedures were approved by the Queen's University Ethics Committee in compliance with the Declaration of Helsinki.

Apparatus

Participants sat in complete darkness 50 cm in front of a 36 cm × 27 cm Dell UltraScan P991 CRT monitor (Dell, Round Rock, TX).

Participants' heads rested on a chin rest that allowed for head roll in the frontoparallel plane. With their heads in an upright position on the chin rest, the interocular midpoint was aligned to the frontoparallel fixation position on the screen. A red 0.625° dot was displayed on the screen (120-Hz refresh rate) using the ViSaGe Visual Stimulus Generator with VSG Toolbox for Matlab (Cambridge Research Systems, Rochester, UK). Movements of both eyes were recorded at 400 Hz using a Chronos head-mounted 3D video eye tracker (Chronos Vision, Berlin, Germany) that was stabilized to the head using a bite bar. Head movements were recorded at 400 Hz using an Optotrak Certus system (Northern Digital, Waterloo, Ontario, Canada) with three infrared diode markers placed on the Chronos helmet. For consistency across camera positions, these helmet markers were calibrated with respect to an external orthonormal axis defined by a set of three orthogonal diodes located either on the wall behind the participant or on the side of the CRT monitor. Screen brightness and contrast settings were adjusted so that participants could not see the edges of the monitor screen in complete darkness, even after 0.5-h dark adaptation.

Procedure

Participants were presented with a series of blocks of trials. A calibration sequence consisting of nine fixation positions (0°, ±5°, and ±10° horizontal and vertical in a grid pattern) was presented on the screen before each session. Participants performed 10 blocks of 50 trials each per session. To avoid dark adaptation across the session, participants rested for a few minutes in between blocks with the lights on. Each participant performed between one and three sessions.

Trials were presented in series of five. The time course showing each trial phase is depicted in Fig. 1C. For each of the first four trials of each series (encoding trials), a red target dot was presented at the center of the screen for 2,000 ms (fixation period). At the start of fixation, participants were verbally instructed to roll their head toward either their left or right shoulder (blue vertical line in Fig. 1C). The initial head roll direction was randomly chosen at the start of each block. After this fixation period, the target dot was extinguished for 300 ms (gap period) and then reappeared, moving from the center at a constant velocity (26.9°/s) in a randomly chosen direction between 1° and 360° for 500 ms (ramp period), then was extinguished. The target ramp direction was kept constant for each series of trials, and participants were informed of this prior to the experiment. During each trial, auditory tones (gray vertical lines, Fig. 1C) indicated to the participant 300 ms before the gap period began and the starts of the gap and ramp periods with the aim of decreasing pursuit latencies (Barnes and Donelan 1999). The trial ended when the target disappeared. Participants were instructed to fixate and pursue the target with their head rolled in the instructed direction and were instructed to maintain approximately the same head roll angle for the first four trials in each series (with no return to upright head roll position between trials).

On the fifth (decoding) trial in each series, participants repeated this exact same protocol, but were instructed to roll their head toward the opposite shoulder during fixation and prior to pursuit. As depicted in Fig. 1A, this change in head roll direction also induced changes in ocular torsion by OCR, thus requiring that velocity memory be updated across these changes for spatially correct anticipatory pursuit. Participants were free to move their head to any chosen eccentricity during encoding and decoding trials, with the resulting variability in the data allowing us to perform regression analyses of the ocular torsion data. A schematic of the experiment in Fig. 1B shows the misalignments between retinal (green), head-centered (blue), and spatial axes (black) arising from head roll (blue shading) and OCR (green shading), which should be accounted for at both encoding and decoding of velocity memory for spatially correct anticipatory pursuit. Directional errors made during the anticipatory pursuit period on this decoding trial showed the extent to which the velocity memory was updated across head roll and ocular torsion changes, thus revealing

details about coding of the pursuit velocity memory and the transformation for anticipatory pursuit (see RESULTS).

Analysis

3D head orientation was computed offline as the difference (using quaternion rotation) between a reference upright position measured at the start of each experimental session and head positions throughout the trials. Participants were instructed to begin the first block of each experimental session with an upright head position before responding to the first verbal head roll instruction.

The 3D eye-in-head position was extracted, horizontal and vertical eye positions calibrated, ocular torsion computed, and saccades detected using the same techniques as those used by Blohm and Lefèvre (2010). Briefly, the 3D eye-in-head position was extracted after each session from the saved images of the eyes using the Iris software (Chronos Vision). This was done using a calibration sequence with the head upright (on the chin rest) for horizontal and vertical eye position, and the eyeball parameters required for the algorithm to extract ocular torsion were determined with the head upright at the start of each block (prior to the first head roll instruction) (Moore et al. 1996). Ocular torsion was computed using the cross-correlation between iris segments across images (Schreiber and Haslwanter 2004). Eye-in-head position was low-pass filtered (autoregressive forward-backward filter, cutoff frequency = 25 Hz) and differentiated twice (weighted, central difference algorithm, width = 5 ms). Saccades were detected using a threshold of $500^\circ/s^2$, as previously done (Blohm and Lefèvre 2010). Smooth pursuit onset was detected with a velocity backward interpolation technique (Badler and Heinen 2006; Blohm and Lefèvre 2010; Carl and Gellman 1987; Krauzlis and Miles 1996). Using an EV threshold of $2 \times SD$ of fixation velocity (maintained over a 30-ms window), we regressed velocity over a 100-ms period following the crossing of this threshold and extrapolated backward to find the velocity intercept time. This time represented the onset of the eye movement. The time window during which pursuit onset was considered anticipatory began at the start of the gap period and ended 75 ms after the ramp onset. We defined the eye movement direction as the direction of the eyes sampled at the end of this 75-ms time window for decoding anticipatory trials (*trial 5*). The 75-ms delay conservatively accounted for visual processing delays after ramp onset, which is estimated to be ~ 100 ms (e.g., Lisberger 2010). We also further accounted for any potential visually guided pursuit that might have occurred 75 ms after target onset by performing each of our analyses using a decoding trial eye direction sampled 50 ms after target onset and obtained qualitatively identical results. For each trial, the head roll measurement was obtained at the end of each trial, and OCR was determined from eye position data at the moment of pursuit onset.

We recorded a total of 5,450 trials from seven participants. Trials containing low onset eye velocities that we assumed to be a result of measurement noise ($<1^\circ/s$), containing blinks or saccades during the gap and ramp periods and prior to pursuit onset were removed. Similarly, trials with head motion at pursuit onset, with inadequate eye tracking data due to the failure of the software to capture the true location of the pupil or measure ocular torsion (usually resulting from pupil dilation with elapsed block time), and those trials missing 3D head measurement data due to obstruction to the view of the camera of the helmet-mounted infrared diodes were removed. Finally, fifth trials during which participants failed to roll their heads toward the opposite shoulder prior to the gap period were also removed. Thus, note that invalid trials were not due to inaccuracies in the eye movements; rather they were excluded due to data acquisition and/or measurement errors. Combined, these trials comprised 26.9% of all trials, leaving 3,986 valid trials. After visually examining all trials in each block for both eyes, we selected which eye recording would be used for further analyses, depending on which provided more valid trials (i.e., better quality eye signals). Of valid trials, we determined the total number of consecutive (i.e., within the same trial series) pairs

of memory encoding and memory decoding trials. We did this by first finding all fifth trials that had anticipatory pursuit onset latencies (see above), then by finding corresponding valid fourth trials. If no valid fourth trial could be found, valid third trials were used instead (6.5% of trial pairs), for a total of 566 encoding-decoding trial pairs. Each participant had from 24 to 210 encoding-decoding trial pairs. For our head-centered updating analysis, we isolated the updating effects by removing outlier trial pairs during which participants exhibited observed head-centered updating angles (U_H) outside the 95% confidence interval (CI) determined by linear regression analysis between change in head roll and observed U_H (for each participant), leaving a total of 510 trial pairs for this analysis.

Detailed regression analysis. To capture the extent to which velocity memory was updated between encoding and decoding trials, we needed to use a parameter that could be directly compared with the change in head roll and to the encoding OCR. The change in eye-in-head direction between encoding and decoding trials captured this effect. If the memory were coded according to the spatial hypothesis (i.e., if all head and eye orientation signals were accounted for by the velocity memory), then this head-centered eye direction change would be directly proportional to head roll and OCR changes. However, if the memory were not coded in a spatial reference frame (i.e., if head or eye orientation signals were not accounted for by the velocity memory), the head-centered eye direction change would not be proportional to the head roll and/or OCR changes. We computed the observed head-centered velocity memory updating (U_H), under the assumption that the encoding eye direction was spatially accurate [i.e., that encoding eye-in-head direction is equal to the encoding target direction in head-centered coordinates ($\theta_{TH,enc}$)]. This assumption was supported by the correlation coefficient between the two parameters on encoding trials across all participants ($n = 510$ trials, $r = 0.74$, $P < 0.0001$), and it was made to eliminate variability in our dataset unrelated to the updating of anticipatory trajectory:

$$U_H = \theta_{EH,dec} - \theta_{TH,enc} \quad (1)$$

where $\theta_{EH,dec}$ is the decoding eye-in-head direction.

The $\theta_{TH,enc}$ was determined by rotating the displayed spatial target direction by head roll. The $\theta_{EH,dec}$ was directly measured using the head-mounted eye tracker. The U_H could be compared with both the required head updating angle (i.e., the angle between decoding head position and encoding head position) and the required ocular torsion compensation (i.e., the angle of encoding OCR) by way of linear regression. Because the head-centered target direction is simply the retinal target direction rotated by the angle of OCR, $\theta_{TH,enc}$ expands (Eq. 3), enabling us to separately analyze head roll and OCR effects (Eq. 2):

$$U_H = \theta_{EH,dec} - (\theta_{TR,enc} + \varphi_{OCR,enc}) \quad (2)$$

with

$$\theta_{TH,enc} = \theta_{TR,enc} + \varphi_{OCR,enc} \quad (3)$$

where the subscript R represents retinal coordinates, and φ_{OCR} represents the ocular torsion angle ($^\circ$). $\theta_{TR,enc}$ is encoding target direction in retinal-centered coordinates; and $\varphi_{OCR,enc}$ is encoding ocular torsion angle.

With $\Delta H = \varphi_{H,dec} - \varphi_{H,enc}$, we obtain our regression equation:

$$U_H \stackrel{?}{=} \beta_1 \Delta H - \beta_2 \varphi_{OCR,enc} \quad (4)$$

where $\varphi_{H,dec}$ and $\varphi_{H,enc}$ represent decoding and encoding head roll angles, and β_1 and β_2 represent the updating gains for head roll change and encoding OCR, respectively. Note that there was no intercept in this regression model.

In our regression analyses, we compared Eqs. 1 and 4 to determine the amount of head roll (β_1) and ocular torsion (β_2) for which velocity memory was updated.

Therefore, if the velocity memory were updated across changes in both head roll and encoding OCR, the regression gains (β_1 and β_2) between the required updating and actual updating would be equal to 1, meaning the memory was in a spatial frame (or in a perfectly updated retinal frame). Conversely, if the velocity memory were not updated, the correlation gains would be equal to 0, meaning the memory was in either retinal or head-centered frame, depending on the presence of OCR compensation.

Because the gain corresponding to OCR updating was not significant in our multiple regression analysis (see RESULTS), we also performed simple regression analyses for each participant across only head roll, based on the regression model in Eq. 5:

$$U_H \stackrel{?}{=} \alpha \Delta H \quad (5)$$

where α represents the simple regression slope corresponding to updating across change in head roll.

To allow us to perform regression analyses on our encoding-decoding trial data (which were initially bimodal), we sign-normalized several parameters based on the encoding head roll direction. By convention, all encoding head rolls originally in the negative CW direction became positive. As a result, all encoding trials had positive head roll values, while all decoding trials (after a switch in head roll direction) had negative head roll values. Accordingly, ocular torsion values changed sign with head roll measurements. Finally, we recomputed the head-centered eye and target directions for these trials by rotating their velocities across the vertical axis (i.e., sign-normalized velocity direction = $180^\circ - \text{original velocity direction}$). Additionally, because we sign-normalized our data, any intercept values found in regular regression analyses were not representative of our data. This is simply demonstrated by the proportional nature of the OCR response; when there is no roll from an upright head orientation, there should be no OCR, by definition. Thus there should be no intercept in a model of its response. Similarly, updating should be proportional to the amount of updating required. When the head roll angle does not change between trials, there should be no updating of velocity memory, by definition. We, therefore, forced the regression fits through the origin. As such, regular regression analysis tests, including using r^2 values to address goodness of fit, were not appropriate for our analyses because the least squares variance was often larger than that of the regression variables. Instead, to address the significance of the slopes, we estimated their 95% CIs, and to address goodness of fit we computed each fit's root mean squared error (RMSE). Additionally, to investigate the validity of our zero-intercept regression model findings, we performed a robust version of our stepwise multiple regression analysis with a free intercept parameter.

Because vertical and horizontal pursuit movements have been found to exhibit differing dynamics (Rottach et al. 1996), we also tested for these effects on our regression results. We did this by binning trial pairs into four 90° bins about the vertical and horizontal axes on the screen (two bins for either vertical or horizontal encoding trial head-centered target directions with edges at 45° , 135° , 270° , and 315°) and repeating our regression analyses. For each target direction bin, regression analysis of the binned data yielded results qualitatively similar to those of the full dataset, indicating that target direction had little to no effect on our results.

OCR compensation analysis. To confirm our updating analysis results, we performed an additional OCR compensation analysis comparing the OCR compensation on encoding and decoding trials to the predicted amounts (assuming an updating of velocity memory for head roll change). Because accurate pursuit during encoding and decoding trials would be required to compensate for the same (encoding) OCR angle, we could use regression analyses to compare these trials to observe the updating of the velocity memory across OCR changes. For both encoding and decoding trials, the required OCR compensation was the opposite (negative) of the angle of OCR. For encoding trials, the observed OCR compensation was the angle

between the measured head-centered eye direction ($\theta_{EH,enc}$) and the computed retinal target direction ($\theta_{TR,enc}$). For decoding trials, the observed compensation was the angle between the measured eye-in-head direction ($\theta_{EH,dec}$) and head-centered target direction ($\theta_{TH,dec}$), rotated by encoding OCR ($\varphi_{OCR,enc}$), such that a regression slope of 1 would indicate perfect OCR compensation, and a slope of 0 would indicate no compensation.

Because the observed OCR compensation data were widespread (encoding SD = 23.1° ; decoding SD = 38.1°) compared with the predicted OCR compensation (measured encoding OCR SD = 2.14°), we utilized robust regression method with a bi-squares weighting function (instead of a standard least squares regression model), which minimized the impact of outliers to our regression fit by weighting them less (for review, see Ronchetti 1997).

Statistical tests. We used one-way ANOVAs to compare trial means between series and paired *t*-tests to compare trials within the same series, while we used unpaired *t*-tests for significance testing of our regression results. We used Bartlett's test for equal variance (for comparing trial variances between series) and *F*-tests of variance (for comparing trials within the same series) to compare variances.

RESULTS

Quantification of Experimental Measures: Typical Trial Series

Figure 2 presents data from an entire typical decoding trial and from the onset of the gap period until trial end for its accompanying encoding (first four) trials (*participant 4, block B, trials 31–35*). Figure 2A shows the evolutions of head roll and OCR (*top row*; black and light blue traces and axes, respectively), eye-in-head position (*pos.*; *middle row*), and eye-in-head velocity (*vel.*; *bottom row*) as the trials in this series occurred. This participant exhibited a consistent head roll angle throughout *trials 31–34* and a typical head roll movement on *trial 35*; in general, participants maintained their head roll angle for the first four trials and rolled their heads smoothly from one shoulder to the other soon after the verbal instruction at the start of the fifth trial. Additionally, OCR remained constant throughout the first four trials of the series, before changing direction along with head roll at the start of the fifth trial, as was also typically the case among participants.

The *middle* and *lower* rows of Fig. 2A present the eye and target positions and velocities, respectively, over the same trial series. In these plots, the thicker lines represent eye tracking data, and the thin lines show target data (after ramp onset at 2.3 s). The dashed lines represent the horizontal component in the frontoparallel plane (*h*), whereas the solid lines represent the vertical component (*v*) and for the velocity traces the thickest, colored lines represent the magnitude of their combined vectors [$\mathbf{h} + \mathbf{v} = (\mathbf{h}^2 + \mathbf{v}^2)^{1/2}$]. Note that in the position row, we omitted the combined position vectors. The gray shaded regions represent the time window during which pursuit was considered anticipatory (see METHODS). Evidenced by the large deviations of eye position and velocity from zero during the head roll change on *trial 35*, participants' eye-in-head position changed to maintain fixation (see zero EV after head roll change). The onset of pursuit movements (including both visually guided and anticipatory movements, as determined using the algorithm described in METHODS) is shown by the color-coded arrows below each velocity trace.

Figure 2B shows the velocity magnitude traces for each trial in the series (*trials 31–35*). For each trial, pursuit onset (in-

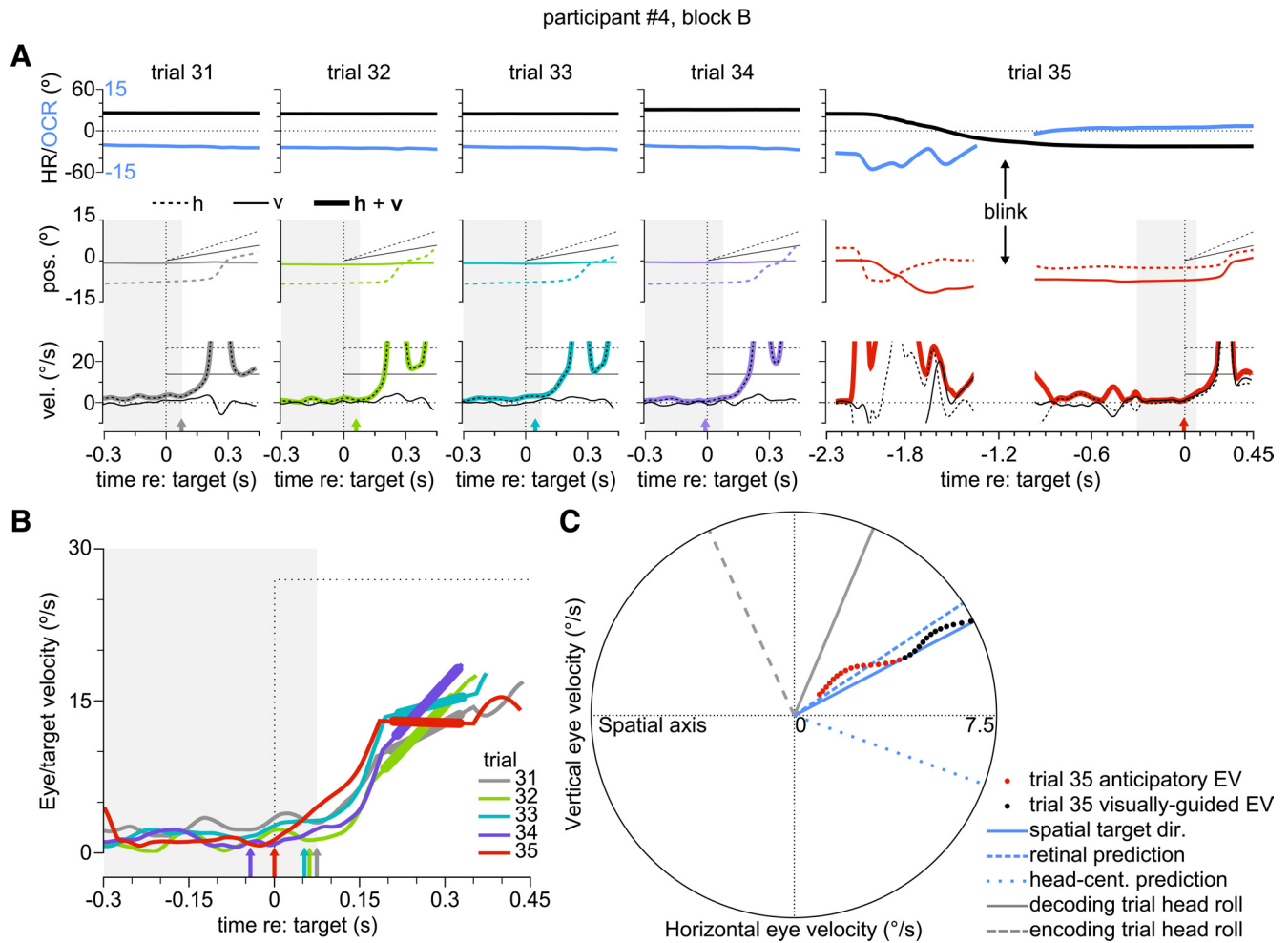


Fig. 2. Typical trial series. *A*: typical trial series (*participant 4, block B, trials 31–35*) HR, OCR, eye position (*pos.*), and eye velocity (*EV*; *vel.*) traces from the onset of the gap period (-0.3 s) and from trial start (-2.3 s) until the trial end for *trials 31–34* and *trial 35*, respectively. Note that we labeled trial timing relative to target onset. *Top row*: spatial HR and OCR, showing consistent HR (black) and OCR (light blue) throughout the first four trials (*trials 31–34*), and a smooth HR transition from clockwise (CW) (negative) to counterclockwise (CCW) (positive) direction with a corresponding rotation of OCR in the opposite direction on the fifth trial (*trial 35*). *Middle row*: eye-in-head position for *trials 31–35*. The dashed lines represent the horizontal component in the frontoparallel plane (*h*), whereas the solid lines represent the vertical component (*v*). Note that we omitted the combined position vectors. On the fifth trial of the series (*trial 35*), we see a change in eye-in-head position due to HR while fixating the target (note that the eye tracker was head-mounted). This plot also shows target position data (thin lines) obeying the same plotting conventions as eye position. For *trial 35*, target data are plotted only after the ramp onset for clarity (even though the target was present at 0° until the gap period onset at -0.3 s). Finally, ramp onset is represented by the vertical dashed black lines, and the gray shaded regions represent the time window during which pursuit was considered anticipatory (see *METHODS*). *Bottom row*: eye-in-head velocity plots (same conventions as position traces) and target velocity information (thin lines, same conventions as position traces). The thickest colored lines represent the magnitude of their combined vectors $[\mathbf{h} + \mathbf{v} = (\mathbf{h}^2 + \mathbf{v}^2)^{1/2}]$. Pursuit onsets (vertical color-matched arrows beneath each velocity plot) are also shown (see *METHODS* for detection protocol). Similarly to what we observed in the eye position trace on *trial 35*, the EV trace shows eye-in-head movements associated with rolling the head while maintaining target fixation. *B*: typical, color-coded EV traces for *trials 31–35* (from gap onset to trial end) merged onto one plot, showing trial-by-trial pursuit onsets (vertical color-matched arrows). Removed saccades across which we interpolated velocity (see *METHODS* for saccade detection and removal protocol) are represented by thick portions of each trace. Note that *trials 32–34* each ended in a saccade (see *A, bottom row* traces), leaving us with no endpoint for velocity interpolation after removal of saccades (thus the velocity traces for these trials terminate early). *C*: spatial plot showing corresponding spatial target direction (solid light blue line), the memorized target direction predicted by a retinal velocity memory, which has been updated across HR changes but not encoding OCR (light blue dashed line; see *METHODS*), the memorized target direction predicted by a head-centered velocity memory, which has been updated across encoding OCR but not HR changes (light blue dotted line; see *METHODS*), and decoding spatial anticipatory (red circles) and visually guided (black circles) pursuit velocity for fifth trial (*trial 35*). The space between each velocity point represents 0.005 s. HR for encoding (gray dashed line) and decoding (gray solid line) trials are also shown. The EV trace for this trial is shown for 210 ms following pursuit onset to maximize visibility of the anticipatory portion of the EV trace.

cluding both anticipatory and visually guided movements) is represented by the color-matched vertical arrows, and bold portions of the traces represent removed saccades (Blohm and Lefèvre 2010). Overlaying the velocity magnitude traces from all five trials and examining the pursuit onset in each (color-matched arrows below traces) reveals a gradual decrease in pursuit onset latency, as expected with repeated target exposures. Inspection of this series of trials reveals the general trend

of building anticipation from the first trial (gray) to the fourth trial (purple), with an increase in latency from the fourth to the fifth trial (red).

Figure 2C is a spatial plot of eye (red and black circles) and target velocities (solid light blue line), as well as encoding (dashed gray line) and decoding head rolls (solid gray line), sampled over the first 210 ms after anticipatory pursuit onset on *trial 35*. The space between each EV

sample represents 5 ms, and red circles represent anticipatory pursuit, whereas black circles represent visually guided pursuit. Also, the target direction prediction based on an encoded retinal target representation (dashed light blue line) and the target direction prediction based on a target representation coded in head-centered coordinates (dotted light blue line) are shown (further described in *Detailed analysis of OCR compensation*). We chose to plot velocity for a few reasons: 1) velocity is what drives smooth pursuit, and it was the parameter we used to detect the onset and direction of pursuit; 2) it reveals the direction of the eyes at any given moment in the movement; and 3) it is preferable to plotting position (which might be more intuitive to interpret) because of the acceleration of the eyes, which would cause the scaling of the plot to be not conducive to examining directional effects.

Quantification of Experimental Measures: OCR and Head Roll

Before analyzing anticipatory eye velocities for directional errors caused by ocular torsion and/or head roll, we wanted to ensure that our paradigm consistently induced both OCR and anticipatory pursuit (Fig. 3). To determine the average amount of OCR induced by head roll, we performed simple linear regressions between sign-normalized (see METHODS) head roll and OCR during paired encoding (purple) and decoding (red) trials. Note that we discarded any trials for which the head position was not stationary at the moment of pursuit onset. Data plotted in Fig. 3A shows the extent of this OCR compensation. The slope of these regressions revealed that OCR compensated for 16% of head roll (gain of -0.16) during encoding trials [$n = 565$ trials; 95% CI: $(-0.17, -0.15)$;

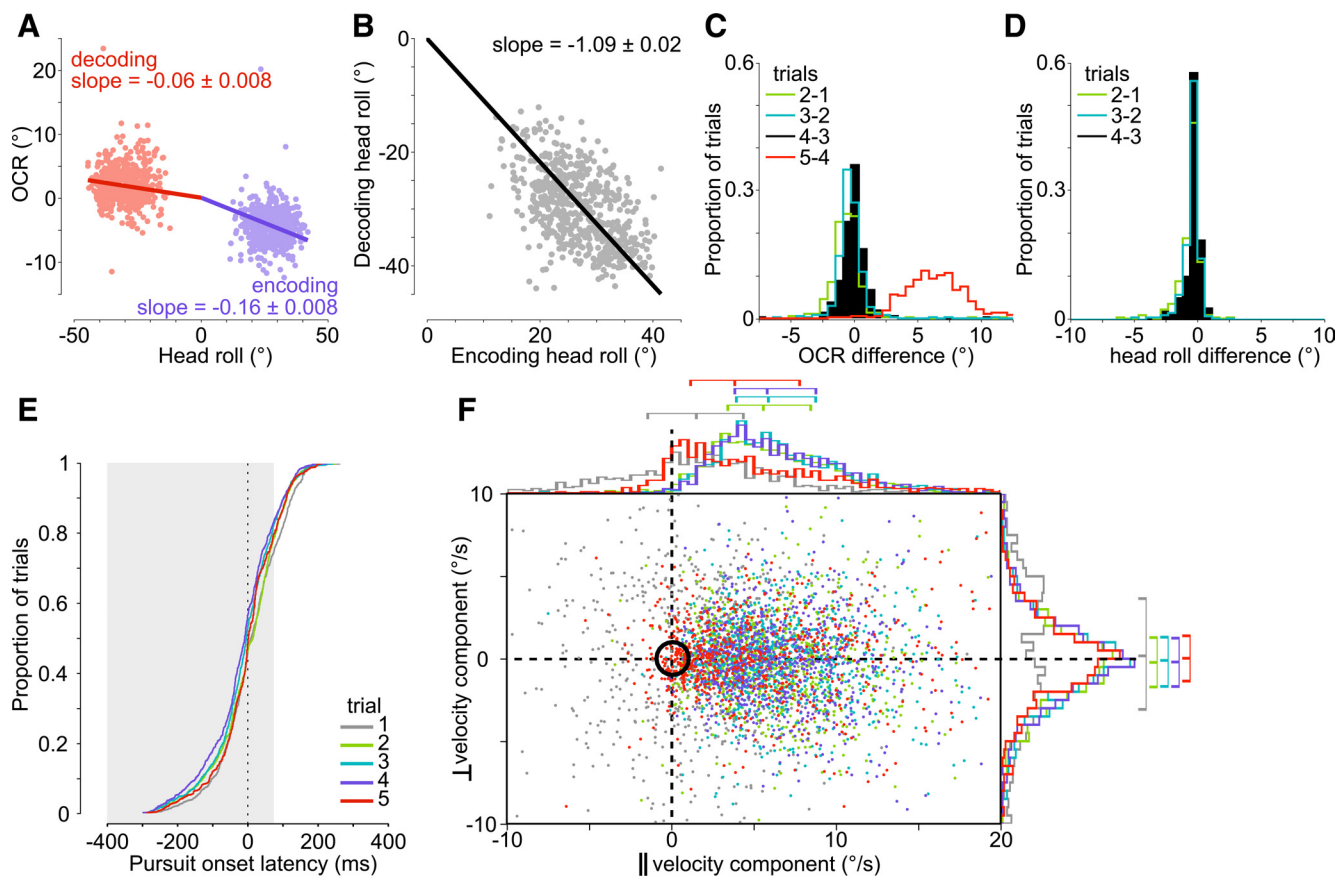


Fig. 3. Quantification of experimental measures. **A:** OCR is plotted against HR for encoding (purple) and decoding (red) trials. The slopes of these regressions revealed that OCR compensated for 16% of HR [slope \pm 95% confidence interval (CI) = -0.16 ± 0.008] during encoding trials [$n = 565$ trials; root mean square error (RMSE) = 2.77°] and 6% of HR (slope \pm 95% CI = -0.06 ± 0.008) during decoding trials ($n = 565$ trials; RMSE = 2.84°). **B:** decoding HR is plotted against encoding HR. Linear regression analysis revealed that decoding HR magnitude was, on average, 9% greater and in the opposite direction (as instructed) from encoding HR (slope \pm 95% CI = -1.09 ± 0.02 ; RMSE = 6.49°). **C:** trial-by-trial OCR variability analysis. We subtracted each HR and OCR measurement from those of the preceding trials within the same trial series and examined the resulting distributions, shown here for the differences between trials 2 and 1 (green), trials 3 and 2 (cyan), trials 4 and 3 (black, filled), and trials 5 and 4 (red). **D:** trial-by-trial HR variability analysis. Similar to C, here we show the deviations in HR angles throughout the first four trials of each series. Here, we only depict changes between trials 1 and 2 (green), 2 and 3 (cyan), and 3 and 4 (black, filled) because those between trials 4 and 5 were comparatively large (typically $> 30^\circ$) and were unimportant for an analysis of the variability of HR from trials 1–4. **E:** pursuit cumulative latency distributions revealing gradual decrease in median pursuit latency from trials 2–4, excluding the first and fifth trials. The gray shaded region represents the window from gap onset to 75 ms after target onset for which any pursuit was considered anticipatory (see METHODS). Median latencies for each trial number were thus anticipatory, as elicited by our task design. **F:** effects of eye speed on eye direction. Here, we compare the component of the eye velocities parallel to the target (i.e., the spatially correct component; \parallel velocity component, abscissa) to that which is perpendicular (i.e., the error component; \perp velocity component, ordinate) across all valid trials to examine the effect of eye speed on directional accuracy. The distributions of each trial's parallel and perpendicular velocity are summarized by the color-matched histograms and corresponding quartiles along the outer edges of the central panel. The data in this panel follow the same color scheme as in E. Note that the trials within the black circle (radius $1^\circ/\text{s}$) were excluded from our updating analyses (see METHODS).

RMSE = 2.77°] and 6% of head roll (gain of -0.06) during decoding trials [$n = 565$ trials; 95% CI: $(-0.07, -0.05)$; RMSE = 2.84°]. The reason for this difference in OCR magnitude between encoding and decoding trials is unclear, but may be related to the stabilization of OCR across each series of trials, an effect which has been observed over prolonged periods (>10 s) of static roll-tilt in humans (Hamasaki et al. 2005). Individual differences in the OCR response occurred across participants during encoding trials in terms of mean magnitude [$F(6) = 5.47, P < 10^{-4}$, corresponding to gains from -0.25 to -0.12]. The variance of the OCR response was also different across participants [$\chi^2(6) = 69.85, P < 10^{-12}$]. During decoding trials, we observed no significant individual differences in mean OCR magnitude [$F(6) = 1.97, P = 0.07$, corresponding to gains from -0.12 to -0.05], but found different variances of the OCR response between participants [$\chi^2(6) = 73.58, P < 10^{-13}$]. This highly variable interparticipant OCR response is consistent with previous evidence (Diamond et al. 1979). We also found no significant overall change in variance of OCR magnitude from encoding trials to decoding trials [$F(6,6) = 1.15, P = 0.87$].

We performed a regression analysis between consecutive (paired) encoding and decoding trials' head rolls (Fig. 3B). The slope of this regression revealed that participants rolled their heads $\sim 9\%$ more (in the opposite direction, corresponding to a gain of -1.09) on decoding trials than on encoding trials for any given encoding-decoding trial pair [mean encoding head roll magnitudes from 18.9° to 33.5° , mean decoding head roll magnitudes from -37.8° to -20.2° , corresponding to gains from -1.12 to -0.94 ; $n = 510$ trial pairs; RMSE = 6.49°; 95% CI: $(-1.11, -1.07)$]. There was unequal interparticipant head roll variability on both encoding and decoding trials [encoding: $\chi^2(6) = 62.23, P < 10^{-10}$; decoding: $\chi^2(6) = 56.80, P < 10^{-9}$], and there were interparticipant differences in mean head roll magnitude for both groups of trials [encoding: $F(6) = 57.96, P < 10^{-10}$; decoding: $F(6) = 132.86, P < 10^{-10}$]. This interparticipant head roll variability was expected as participants were free to roll their head as they preferred. This variability in the data allowed us to reliably characterize head roll tendencies using regression analysis. We found no significant overall change in head roll variability from encoding trials to decoding trials [$F(6,6) = 0.60, P = 0.54$].

Before using head roll and OCR signals to make any determinations about the reference frame of the encoded velocity memory, we wanted to see how consistent head roll and OCR were while the memory was being coded throughout each trial series. If these signals were being coded within a velocity memory, their reliabilities during encoding might influence our ability to detect them upon decoding. On the other hand, the consistency of head roll and OCR on encoding trials might be irrelevant, as the brain could presumably use the visually guided portion of the pursuit movement to store velocity information, or they might already be included in the memory itself. Regardless, with our assumption that the third trials of each series could be used as the encoding trial paired with fifth trials (in cases for which the fourth trials were invalid, see METHODS), it was important that head roll and OCR were constant between trials 3 and 4.

We subtracted each head roll and OCR measurement from those of the preceding trials within the same trial series and examined the resulting distributions, shown as histograms in

Fig. 3, C and D. Figure 3C shows the results of this analysis for the differences in measured OCR angles between trials 1 and 2 (green), between trials 2 and 3 (cyan), between trials 3 and 4 (black, filled), and between trials 4 and 5 (red). A group-level comparison of these distributions revealed that OCR was not constant throughout the first two trials of each series [for trials 1 and 2: mean = -0.60° , SD = 1.83° , $t(6) = -4.35, P < 0.01$], although the distribution was clustered near zero. However, we found no significant difference in OCR between trials 2 and 3 [for trials 2 and 3: mean = -0.47° , SD = 2.15° , $t(6) = -1.34, P = 0.23$] or between trials 3 and 4 [for trials 3 and 4: mean = -0.01° , SD = 2.14° , $t(6) = -1.37, P = 0.22$], supporting our decision to use either the fourth or third trial as the encoding trial in subsequent analyses. Despite the apparent progressive narrowing of each distribution, group-level comparisons of the variance of each distribution revealed that there was also no significant change in the variance from trials 1–4 [trials 1 and 2 compared with trials 2 and 3 distributions: $F(6,6) = 0.40, P = 0.29$; trial 2 and 3 compared with trial 3 and 4 distributions: $F(6,6) = 1.09, P = 0.92$]. Qualitatively, the changes in OCR became smaller with each trial, as depicted by the progressively decreasing absolute means of each distribution. Also, differences in OCR induced by the change in head roll from trial 4 to 5 were consistently in the positive direction (as expected) and deviated from those seen between the other trials of the series, as evidenced by minimal overlap between the distributions [for trial 5 to 4: mean = 6.22° , SD = 3.19° , $t(6) = 17.4, P < 10^{-5}$; comparing trial 4 to 3 and trial 5 to 4 distributions: $t(12) = 16.2, P < 10^{-8}$].

Similarly, Fig. 3D shows the deviations in head roll angles throughout each trial series. Here, we only depict changes between trials 1 and 2 (green), 2 and 3 (cyan), and 3 and 4 (black, filled) because those between trials 4 and 5 were comparatively large (typically $>30^\circ$) and were unimportant for determining head roll constancy across trials 1–4. Head roll was relatively consistent throughout the first four trials of each series, as evidenced by distributions close to zero; however, the means of these distributions were slightly negative [for trials 1 and 2: mean = -0.65° , SD = 1.00° , $t(6) = -2.72, P < 0.05$; for trials 2 and 3: mean = -0.46° , SD = 0.72° , $t(6) = -2.72, P < 0.05$; and for trials 3 and 4: mean = -0.37° , SD = 0.69° , $t(6) = -2.78, P < 0.05$]. The slightly negative skew of the distributions indicates that any changes in head roll were typically small decreases in roll magnitude from trial to trial. Also, despite the apparent progressive narrowing of the histograms, we detected no significant change in variability between any of the encoding trials [trial 1 and 2 compared with trial 2 and 3 distributions: $F(6,6) = 3.35, P = 0.17$; trial 2 and 3 compared with trial 3 and 4 distributions: $F(6,6) = 1.75, P = 0.51$].

Quantification of Experimental Measures: Anticipatory Response

Overall, participants' anticipatory responses followed an expected "build-up" trend within each trial series. Figure 3E shows the cumulative distribution across all participants and all trial sets for each trial's pursuit onset latency and its relation to the predefined, shaded anticipatory pursuit time window (see METHODS). In Fig. 3E, this increasing anticipatory trend between trials 2 and 4 can be seen in the leftward shift of their

cumulative plots; participants increasingly anticipated the target velocity with repeated exposures, in agreement with previous experiments (Knox 1996, 1998; Wells and Barnes 1998). Increased anticipation was not apparent between the first and second trials of each trial series; in fact, pursuit onset latencies increased from *trial 1* (*trial 1* median latency = 1.01 ms) to 2 [*trial 2* median latency = 6.07 ms; $t(1,507) = 2.01, P < 0.05$]. This was likely because first trials' eye movements were often anticipatory for the previous trial series' target direction. Thus a new target direction had to be learned for the rest of the trial series (*trials 2–5*), resulting in latencies that were longer than those of the first trial of each series. Pursuit latencies decreased from *trial 2* to 3 [*trial 3* median latency = -11.77 ms; $t(1,710) = 2.15, P < 0.05$] and from *trial 3* to 4 [*trial 4* median latency = -16.60 ms; $t(1,748) = 1.99, P < 0.05$]. On the fifth trial, latencies were slightly longer than on the fourth trial [*trial 5* median latency = -5.82 ms; $t(1,598) = -3.95, P < 10^{-4}$], which might be attributed to the increase of uncertainty about target motion after head roll change, but also may be partially explained by our pursuit onset detection algorithm. Because we based the detection of pursuit onset on the deviation of the eye-in-head velocity from the baseline variability of fixation velocity (see METHODS), this threshold was higher (and thus was reached later) on trials with a change in head roll (i.e., the first trials of each block and decoding trials) due to changes in eye-in-head position required to maintain fixation. However, group-level comparisons of each participant's average pursuit onset latencies revealed no significant changes in pursuit latency as the trials progressed (with 12 degrees of freedom, all P values > 0.05), but there was a significant decrease in latencies between *trials 1* and 4 [$t(12) = 2.68, P < 0.05$]. In general, our task elicited anticipatory pursuit on a large percentage of trials, as shown by the large proportion of each curve lying within the anticipatory time window (see Fig. 3E).

Quantification of Experimental Measures: Effects of Eye Speed on Pursuit Direction Variability

One aspect of the data that we have yet to consider is how the magnitude of the EV, or eye speed, affected the variability of eye direction. Importantly, if the speed of the eyes influenced the variability of their direction, then attributing any changes in eye direction between encoding and decoding to head roll changes and/or OCR would be problematic. In Fig. 3F, we compare the component of the eye velocities parallel to the target (i.e., the spatially correct component; \parallel velocity component, abscissa) to that which is perpendicular (i.e., the error component; \perp velocity component, ordinate) across all valid (i.e., including both anticipatory and visually guided pursuit) trials to examine the effect of eye speed on directional accuracy. Note that the trials within the black circle (radius $1^\circ/\text{s}$) were excluded from our updating analyses (see METHODS). We see that the distribution of velocities for first trials (gray points and histograms) is dispersed relative to its second (green), third (cyan), fourth (purple), and fifth (red) trial counterparts. This finding is expected, as during our experiment participants often exhibited anticipatory pursuit related to the previous trial series on the first trial of the each series (which was in a randomly selected, different direction).

The quartiles for the velocity distributions on *trials 2–4* (color-matched ticks adjacent to histograms) reveal that the

parallel velocity component typically became larger as each series progressed from *trial 2* to 3 [*trial 2* median = $5.58^\circ/\text{s}$ and *trial 3* median = $5.88^\circ/\text{s}$, $F(1701) = 4.38, P < 0.05$] but not from *trial 3* to 4 [*trial 4* median = $5.81^\circ/\text{s}$, $F(1739) = 0.01, P = 0.91$]. On *trial 5*, the parallel velocity component typically decreased [*trial 5* median = $3.84^\circ/\text{s}$, $F(1591) = 62.1, P < 0.01$]. Contrastingly, we found no significant change in both the means and variances of the perpendicular components from *trial 2* through 5 [mean comparisons: *trials 2* and 3 $F(1701) = 0.04, P = 0.83$; *trials 3* and 4 $F(1739) = 0.02, P = 0.89$; *trials 4* and 5 $F(1591) = 2.43, P = 0.12$; variance comparison: $\chi^2(3) = 2.89, P = 0.41$].

As an additional measure of the effects of eye speed on eye direction, we repeated each of our main analyses with trials exhibiting either above- or below-median decoding trial eye speeds, and obtained qualitatively identical results compared with those of the full dataset.

Anticipatory Directional Error Analysis

As a first step in our main analyses, we quantified any directional errors that occurred during velocity memory-driven anticipatory decoding trials by comparing their accuracy to those of their encoding trial counterparts. To directly compare directional accuracy between each trial series, we performed a regression analysis of eye direction in spatial coordinates against target direction in spatial coordinates. If updating errors occurred as a result of change in head roll or OCR, then compared with encoding trials this analysis should reveal an increase in directional errors on decoding trials.

Figure 4A shows the distributions of eye direction compared with target direction for paired encoding (purple) and decoding (red) trials. For clarity, the data were binned (10° width) according to the spatial target direction, and within each bin we computed the average spatial target direction and average spatial eye direction, represented by the solid, color-matched lines. Plotted perpendicular to the line of unity are the spatial error histograms for encoding (purple) and decoding trials (red). While both regressions had slopes close to unity (1.02 for encoding and 0.97 for decoding), anticipatory decoding trials displayed a significant increase in the variability of pursuit direction [$F(562,564) = 0.34, P < 10^{-10}$], i.e., on average, pursuit during both trials is spatially accurate, but there is an increase in error variability that occurs upon decoding this velocity memory. When comparing participant-by-participant spatial error means, we did not detect a significant change in error means [$t(12) = -0.55, P = 0.60$] or in error variance [$F(6,6) = 0.93, P = 0.93$].

We then determined whether the increase in error variability from encoding to decoding trials was consistent for each participant. In Figure 4B, we plotted each participant's mean error for each trial pair (error bars represent SD). The mean error remained the same from encoding to decoding for all participants, except one [*participant 2*, marked with “†”, $t(80) = 2.03, P < 0.05$]. However, we found an increase in anticipatory directional variability for four of seven participants (points marked with “*”, F -statistics between 0.11 and 0.46, each participant's degrees of freedom > 37 and each $P < 0.01$, except *participant 6*, $P < 0.05$). Since these data include both CW and CCW head roll directions, it could be that the added variability is a result of the combination of two popu-

lations of anticipatory trajectory directions resulting from a systematic updating error related to the direction of head roll. Alternatively, this increase in error variability could have simply been due to added uncertainty in the movement plan as a result of the change in head roll direction.

To determine the source of added variability, we separated the data depending on head roll direction, either CW or CCW

(by convention CW was negative). We then computed the compensation error for each trial by subtracting the spatial target direction from the measured spatial eye direction (such that complete updating across head roll and OCR would result in a compensation error value of 0 and an undercompensation across head roll, and OCR would result in a compensation error value with a sign opposite to the sign of the head roll direction). We plotted these distributions for encoding (Fig. 4C) and decoding trials (Fig. 4D) and for each head roll direction (color shading is CW and black outline is CCW). The compensation error distribution means across all participants and trial pairs for CW and CCW trials (arrowheads in Fig. 4D) did not differ significantly from each other for encoding trials [$t(12) = 1.01$, $P = 0.33$, $\text{mean}_{\text{CW}} = 0.71^\circ$ and $\text{mean}_{\text{CCW}} = -4.79^\circ$], but did differ on decoding trials [$t(12) = 2.63$, $P < 0.05$, $\text{mean}_{\text{CW}} = 6.09^\circ$ and $\text{mean}_{\text{CCW}} = -7.53^\circ$]. The direction-specific significant difference between the means of the decoding trial distributions hints at a systematic error related to changes in head roll and/or OCR. The observation that the signs of decoding trial compensation error distribution means correspond to the opposite of the head roll direction (i.e., that the actual compensation direction was opposite the required direction) suggests that there was either an incomplete updating (undercompensation) across head roll changes, an overcompensation for encoding OCR, or both. While the differences in the eye direction distributions could be due to a systematic error related to head roll direction, we also observed an increase in eye direction variability from encoding to decoding trials for CCW-CW head roll pairs [$F(6,6) = 0.15$, $P < 0.05$], and a nearly significant increase for CW-CCW head roll pairs [$F(6,6) = 0.18$, $P = 0.06$], which might contribute to the differences in CW and CCW eye directions on decoding trials, although the reason for this increase in variability is unclear.

To this point, we have shown that, not only did our paradigm consistently induce OCR, but also it consistently elicited anticipatory pursuit. Our analyses have also suggested that participants' change in head roll (and OCR) between encoding of velocity memory and its decoding for anticipatory pursuit on fifth trials contributed to systematic errors related to updating the velocity memory across these changes. In the following sections, we will examine the contributions of the head roll change and the encoding OCR to these errors in more detail.

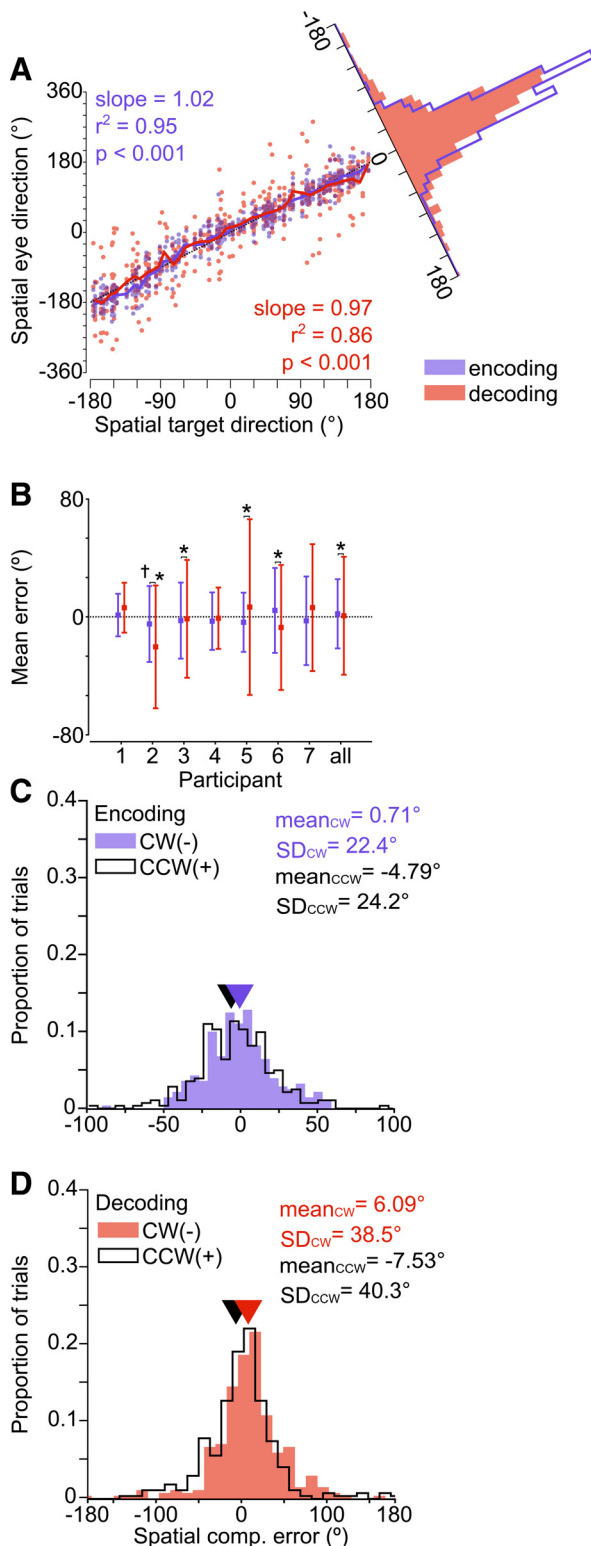


Fig. 4. Spatial accuracy of encoding and decoding trials. **A**: spatial eye direction plotted against spatial target direction, for encoding (purple) and decoding trials (red), with inset error histogram perpendicular to the unity line. For clarity, average eye direction is plotted against average target direction over 10° bins as a solid, color-matched line. On average, we observed spatially accurate pursuit during encoding and decoding trials (both slopes close to 1) but an increase in direction variability on decoding trials [$F(562,564) = 0.34$, $P < 10^{-10}$]. **B**: individual participant and overall mean errors. Asterisk (*) indicates a significant increase in error variance (F -test, $P < 0.01$) from encoding trials to decoding trials (participants 2, 3, 5, and 6), while the dagger (†) indicates a significantly different mean error (paired t -test, $P < 0.05$) between encoding and decoding trials (participant 2 only). Each participant had from 24 to 210 encoding-decoding trial pairs. **C**: encoding trial HR-separated compensation error histograms. CW HR trials are plotted in color, while CCW HR trials are plotted as black outlines. Color-matched text represents corresponding mean compensation error and SD, and arrowheads represent the mean compensation error. **D**: like in **C**, the decoding trial HR separated compensation error histograms are plotted. Plotting conventions are identical to **C**.

Updating Analyses

Our experimental paradigm allowed us to determine the reference frame of velocity encoding and decoding by dissociating the effects of head roll and ocular torsion signals at each stage. Spatially accurate anticipatory pursuit requires that the velocity memory compensates for the extraretinal signals, causing these geometrical misalignments at encoding, and that the memory be updated prior to decoding. As such, we found the amount of compensation that occurred between memory encoding and decoding for changes in head roll and for encoding OCR, respectively. We did this by determining the observed updating and comparing to the required amounts for head roll changes and for encoding OCR in the following sections. Note that we did not test the effect of decoding OCR on anticipatory pursuit, as ocular torsion signals do not affect horizontal and vertical motor commands, but only influence retinal input, which is absent during the anticipatory responses. Using the amounts of head and eye orientation changes for which the velocity memory was updated, we could delineate the memory's reference frame, as described hereafter.

Accounting for head roll changes and encoding OCR. We performed stepwise multiple regression analyses for each participant to determine the amount of updating across head roll changes and encoding OCR. First we computed the multiple regression gains associated with updating velocity memory for both change in head roll and encoding OCR (see Eq. 4 in METHODS). A full updating of velocity memory across extraretinal head and eye changes would correspond to the memory being coded in spatial coordinates (spatial hypothesis; all signals are accounted for during the updating). However, insignificant updating across either parameter would suggest that the memory was coded in either head-centered or retinal coordinates (depending on the presence of OCR compensation).

Figure 5 shows each participant's head roll (β_1) updating gains for our multiple regression analysis (black boxes; error bars represent 95% confidence intervals). Also shown are the predicted gains corresponding to if the anticipatory velocity was decoded in spatial coordinates (dashed horizontal), or if the velocity memory was decoded in either retinal or head-

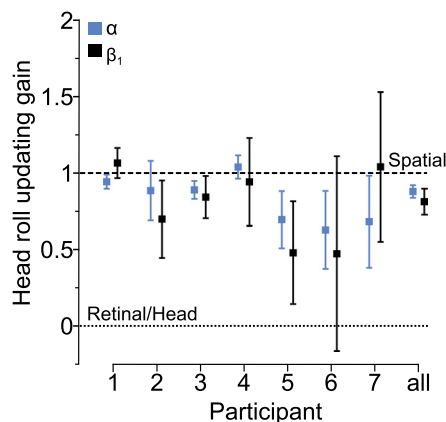


Fig. 5. Updating gains for HR changes. Individual participant and overall head-centered updating gains across HR changes for multiple regression analysis and simple regression analysis are shown. Multiple regression gains across HR (β_1 , black) and simple regression gains across HR (α , light blue), the spatially updated (dashed line; gain = 1) and not updated (dotted line; gain = 0; see METHODS) horizontals are also shown. Error bars represent the 95% CI associated with each gain value.

centered coordinates (dotted horizontal). Across all participants and trial pairs, this multiple regression analysis (see Eq. 4 in METHODS) revealed that, on average, the velocity memory was updated for 81% of head roll change, but not significantly updated for encoding OCR [$n = 510$ trial pairs, model RMSE = 27.6° , model $P < 0.0001$; head roll: gain = 0.81, 95% CI: (0.72, 0.89); OCR: gain = -0.88 , 95% CI: (-1.85 , 0.10)]. Group-level analyses on these multiple regression fits revealed that head roll gains (β_1) were both significantly different from zero [$t(6) = 8.44$, $P < 0.001$] and not significantly different from one [$t(6) = -2.28$, $P = 0.06$]. In contrast, OCR gains (β_2) were not significantly different from zero [$t(6) = -0.23$, $P = 0.83$]. Note that we do not show the updating gains for OCR (β_2) in Fig. 5.

Because OCR gains were not significant, we removed the OCR parameter from the model and then performed a simple regression analysis in which we compared the observed head-centered updating (U_H) with only the change in head roll angle (see Eq. 5 in METHODS). This is a requirement of stepwise regression procedure, because adding a variable to a regression model (regardless of significance) always changes the regression results of significant dependent variables. We show the resulting simple regression analysis gains in Fig. 5 (light blue boxes; error bars represent each 95% CI). This regression analysis revealed that, on average, the velocity memory was updated for 87% of head roll change [corresponding to a gain of 0.87, 95% CI: (0.83, 0.92), $P < 0.0001$]. Group-level analysis revealed that participants' head roll gains (α) were not only significant [$t(6) = 14.0$, $P < 10^{-5}$] but also smaller than one [$t(6) = -3.12$, $P < 0.05$], possibly indicating that the brain might not fully account for changes in head orientation when updating velocity memory. We also performed a robust version of our stepwise multiple regression analysis with a free intercept parameter. Group-level analysis revealed results which were qualitatively similar to our main regression analysis, with a final, significant head roll gain of 1.06 [SE = 0.11; $t(6) = 4.47$, $P < 0.01$], which was not significantly different from 1 [$t(6) = 0.029$, $P = 0.98$]. Using this analysis, we found no significant effect of OCR [$t(6) = -0.136$, $P = 0.897$], no significant interaction effects [$t(6) = -0.082$, $P = 0.937$], and no significant intercept value [$t(6) = 1.47$, $P = 0.192$]. Thus the findings of our regression analyses suggest that velocity memory was only updated for head roll changes, and this updating might have been incomplete. Also, because we could not detect any updating for an OCR signal, these results suggest that this velocity memory is encoded retinally. To confirm if a retinally encoded (and not head-centered) velocity memory does in fact drive anticipatory pursuit, we next investigated the influence of encoding OCR on anticipatory decoding trial trajectories in greater detail.

Detailed analysis of OCR compensation. For the retinal hypothesis to hold true, anticipatory errors should fit its predictions. If a velocity memory were encoded without an OCR signal, anticipatory trajectories on decoding trials after changes in head roll and OCR should contain systematic directional errors proportional to the OCR present at memory encoding (but not proportional to head roll). To more closely examine the error added by encoding OCR on a trial-by-trial basis, we computed the anticipatory direction prediction with updating of a retinal velocity memory across head roll changes (i.e., the encoding retinal target projection rotated by head roll change)

and compared it to the true anticipatory eye trajectories. Figure 2C shows a typical decoding trial (*participant 4, block B, trial 35*) anticipatory EV (red circles), spatial target velocity (solid light blue line), and this retinal prediction rotated by head roll (dashed light blue line). Note that the space between each EV sample represents 5 ms, and this plot shows EV for the first 210 ms after pursuit onset. Qualitative inspection of this trial suggests that EV is biased in the direction of the retinal prediction for target direction during anticipatory pursuit and corrected toward being spatially accurate during visually guided smooth pursuit (black circles).

We compared this required OCR compensation to the amount of OCR for which the brain compensated for paired trials and for additional subsets of encoding trials to test if eye velocities satisfied the requirements of the hypothesis for a retinal velocity memory updated only with head roll. The hypothesis predicts that, under constant head roll and OCR, encoding trial pursuit, whether visually guided or anticipatory, should be spatially accurate, showing compensation for OCR (Blohm and Lefèvre 2010). This is true for anticipatory encoding trials because there is no explicit requirement for participants to use an OCR signal during these trials to achieve spatially accurate movements; when maintaining a constant head roll (i.e., no rotations of the retinal projection due to changes in OCR), the pursuit system can essentially learn the eye-in-head direction required to match the constant retinal input prior to its appearance. In contrast, on decoding trials following those encoding trials (after the head roll change), there should be no compensation for encoding OCR, as the retinal hypothesis predicts that there should be no eye-in-head orientation information encoded to memory. The results of a robust regression fit (see METHODS) for encoding anticipatory (second, third, and fourth) trials indicates that OCR was accounted for by anticipatory encoding trial trajectories, as expected ($n = 2,157$ trials, slope = 1.00, RMSE = 21.7°, $P < 10^{-25}$).

After quantifying the compensation for OCR in anticipatory encoding trials, we examined how this compensation changed across head roll changes by performing this regression analysis for pairs of encoding and decoding trials. In Fig. 6, we show the predicted and actual OCR compensation data (gray points), the locations of the average data bins (colored boxes and error bars), the results of these regression analyses, and their comparisons to the line of unity (dashed black lines). Similar to the anticipatory encoding case, encoding trials composed of both anticipatory and visually guided pursuit showed significant OCR compensation (Fig. 6A, purple line; $n = 525$ paired trials, slope = 1.08, RMSE = 22.6°, $P < 0.05$). When we performed this fit using the paired decoding anticipatory trials (Fig. 6B, red lines), we found no significant compensation for encoding OCR ($n = 525$ paired trials, slope = -0.18, RMSE = 29.0°, $P = 0.76$), indicating that the decoding anticipatory pursuit velocity did not account for encoding OCR. Finally, a simple linear regression analysis confirmed that the lack of OCR compensation could not be attributed to effects of head roll change (all participants $P > 0.05$).

Therefore, decoding trials showed no evidence of compensation for OCR. In summary, our results show that the velocity memory for anticipatory pursuit is updated across head roll changes, and that the eye's torsional component is not a part of

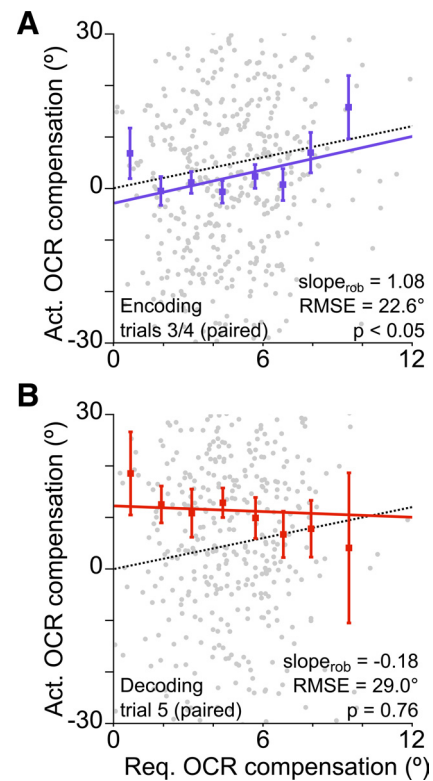


Fig. 6. OCR compensation analysis for encoding-decoding trial pairs. Required and observed (actual; Act.) OCR compensation are represented by gray data points for encoding (purple; A) and decoding (red; B) trial pairs. Color-matched error bars represent SEM and are located at each bin's mean required and mean observed compensations. Bin width is 1.25°, and bins containing 10 or fewer trials were omitted from the error bar plots. The dotted black lines in each panel represent the line of unity. A: we found a significant correlation between the required OCR compensation and the observed OCR compensation on paired encoding trials [purple line; paired third or fourth trials; robust slope (slope_{rob}) = 1.08, RMSE = 22.6°, $P < 0.05$]. B: in contrast, we found no significant correlation between the required ocular torsional compensation and the observed ocular torsional compensation on decoding anticipatory paired trials (red line; paired fifth trials; slope_{rob} = -0.18, RMSE = 29.0°, $P = 0.76$).

this velocity memory, implying that the directional component of the memory is encoded in retinal coordinates.

DISCUSSION

We tested 1) in which reference frame the velocity direction memory for anticipatory pursuit was coded; and 2) whether the velocity memory was updated accurately across changes in head roll and ocular torsion. To do this, we made specific predictions about the required spatial compensation across changes in head roll and ocular torsion and computed the amount of updating for each using anticipatory pursuit movements. We found that anticipatory pursuit accounted for changes in head roll, but not for encoded ocular torsion. This implies that velocity memory could not have been coded in a head-centered or spatial frame of reference, because these possibilities would require complete compensation for ocular torsion (since the extraocular muscles are head-fixed and control the 3D eye-in-head position). Rather, the velocity memory was in a retinal reference frame, as there was no information about the torsional eye-in-head position encoded in the velocity memory. Consequently, when computing the anticipatory command, the pursuit system relied on a velocity memory that

lacked the necessary torsional eye position signals for a spatially correct transformation. We, therefore, propose that the brain integrated a 2D retinally encoded velocity memory with past and current 3D sensory information about the head in space to produce an anticipatory pursuit command.

Our finding that velocity memory for anticipatory pursuit is coded in a retinal frame disagrees with the idea that velocity memory could be encoded using an efference copy of the pursuit motor command, or coded in a head-centered frame (Barnes and Asselman 1991; Barnes and Collins 2008). This idea was based on studies in which observed anticipatory pursuit velocities were indistinguishable from those during visually guided pursuit (Barnes and Asselman 1991; Barnes and Collins 2008). Also, our results indicate that velocity memory is updated across head roll changes using a current estimate of head roll and a vestibular memory of encoding head roll, contrary to a head-free anticipatory pursuit model proposed by Ackerley and Barnes (2011), which only accounts for real-time head (and eye) geometry. This previous work, however, did not distinguish between the encoding and decoding of velocity memory as we did here using head and eye position changes. If the encoded memory were an efference copy of the motor command, it would be coded in head-centered coordinates, because the extraocular muscles are head-fixed. Thus an OCR signal would be encoded within this memory (as ocular torsion is also controlled by the extraocular muscles), resulting in a full compensation for encoding OCR during the decoding trials of our paradigm (Blohm and Lefèvre 2010). Because we found that anticipatory pursuit does not compensate for encoding OCR, we propose that velocity memory is encoded using retinal information rather than motor planning information.

Another consideration that may reconcile our findings with those of previous work (Barnes and Asselman 1991; Barnes and Collins 2008) is the fact that these previous experiments were designed to investigate the storage of speed information for anticipatory pursuit, whereas we only investigated the storage of direction information for anticipatory smooth pursuit. Importantly, there is some evidence that the mechanisms underlying each are dissociated. Kowler (1989) found that participants could voluntarily change the direction of anticipatory pursuit movements in response to a cue, and Jarrett and Barnes (2001) found that participants could change the direction of anticipatory pursuit movements (by 180°) while maintaining target-dependent speed scaling, without having previously observed the new motion direction. Presumably, it might be beneficial for the brain to store speed information in a head-centered reference frame, as theorized by efference copy models (Ackerley and Barnes 2011; Barnes and Asselman 1991; Barnes and Collins 2008), rather than in a retinal frame. This is because the speed of the target on the retina is not constant after the initiation of pursuit movements, therefore requiring that an ongoing estimate of EV be used to reconstruct the required eye-in-head direction. Contrastingly, the retinal direction is constant during pursuit movements to ramp targets, allowing for this aspect of velocity memory to be stored using only retinal information.

Combined with previous work (Balliet and Nakayama 1978; Curthoys et al. 1991; Dieterich and Brandt 1993; Fiehler et al. 2010; Goonetilleke et al. 2008; Haustein and Mittelstaedt 1990; Henriques et al. 1998; Nakayama and Balliet 1977; Pavlou et al. 2003; Poljac et al. 2005; Wade and Curthoys

1997; Zink et al. 1998), our findings raise questions about the exact role of retinal representations in visuospatial memory and perception. Not only have the positions of remembered targets been shown to be encoded in a retinal reference frame (Fiehler et al. 2010; Henriques et al. 1998), but also subjective postural and visual judgments have been shown to be biased by the direction of the retinal stimulus projection (Balliet and Nakayama 1978; Curthoys et al. 1991; Dieterich and Brandt 1993; Haustein and Mittelstaedt 1990; Nakayama and Balliet 1977; Zink et al. 1998) as have the perception of stimuli orientations (Goonetilleke et al. 2008; Pavlou et al. 2003; Poljac et al. 2005; Wade and Curthoys 1997), suggesting that retinal signals could also be the primary basis for perceptual judgments. However, why a retinal representation would be used for these tasks rather than, for example, a spatial representation (which would provide consistent spatial target information across any postural changes) is unclear. One possibility could be that a retinal representation is coded at a higher fidelity than a representation that had to be transformed from a retinal frame to a spatial frame under conditions of head roll (Burns et al. 2011). The brain might use the less variable retinal representation, as the brain has been shown to weigh reliable sensory signals more heavily than variable ones during reference frame transformations (Burns et al. 2010), but the true reason for basing visuospatial memories and perceptual decisions on retinal representations remains to be investigated.

Hypothetical Underlying Neurophysiology

These findings lead us to posit that sensory signals coded within a memory store to drive anticipatory pursuit do not undergo a spatially accurate visuomotor transformation at any point during the production of the motor command. Instead, there was only an updating of this memory across changes in head roll (and not across changes in OCR). Thus the neural mechanisms underlying the encoding, updating, and decoding of velocity memory for anticipatory pursuit are presumably distinct from those underlying the 3D visuomotor transformation for visually guided pursuit (Blohm and Lefèvre 2010). Our findings indicate that the neural circuitry involved would have to maintain persistent activities representing retinal velocity and head roll between pursuit movements. Blohm and Lefèvre (2010) recently hypothesized that neurons in the medial superior temporal (MST) area possess the ideal connectivity and activation characteristics to compute the velocity transformation for visual pursuit; however, not only has this area been shown to encode in suparetinal coordinates, i.e., head-centered or spatially/world-centered (Fujiwara et al. 2011; Inaba et al. 2007, 2011), but also there is no evidence of MST having persistent activity during prestimulus delay periods in anticipatory pursuit tasks (Kurkin et al. 2011; Shichinohe et al. 2009). These limitations make MST an unlikely location for the velocity memory encoding and updating for anticipatory pursuit.

To resolve this issue, there are at least two possible hypothetical solutions: 1) either that MST does not perform the transformation from retinal to head-centered pursuit coordinates, and rather the transformation occurs in a structure downstream of MST in the pursuit circuitry (e.g., superior colliculus, brain stem, or cerebellum); or 2) that a distinct

neural pathway executes the transformation of signals for visually driven vs. anticipatory pursuit.

In support of the first hypothesis, many studies have pointed to the cerebellum because of its involvement in motor learning and in predictive pursuit tasks (Cerminara et al. 2009; Kettner et al. 1997; Medina and Lisberger 2008, 2009; Suh et al. 1997, 2000). Cerebellum has the ability to encode and decode the timing and target trajectories for predictive pursuit (Cerminara et al. 2009; Kettner et al. 1997; Medina and Lisberger 2008, 2009; Suh et al. 1997, 2000), and partial ablations of the cerebellum cause deficits in smooth pursuit and VOR adaptation (Rambold et al. 2002). To our knowledge, no electrophysiological evidence for retinal neuronal reference frames exists in cerebellar neurons, therefore making it unclear whether cerebellum could encode and maintain a retinal velocity memory. There is, however, evidence from cerebellum that inertial signals can be incorporated from vestibular afferents into motor plans (Shaikh et al. 2004; Yakusheva et al. 2007), potentially supporting an updating of a velocity memory across head roll changes.

In support of the second hypothesis, one possibility is that there exist two parallel projections within the pursuit circuitry to the brain stem, one originating from MST and the other from the frontal eye field (FEF) (Nuding et al. 2008). Nuding et al. (2008) suggested that the MST pathway serves as the basic circuit for maintaining an ongoing pursuit movement, while an FEF pathway is responsible for the dynamic gain control of pursuit (Nuding et al. 2008; Tanaka and Lisberger 2001, 2002a, 2002b). FEF is also thought to be involved in predicting the trajectories of moving visual targets (Barborica and Ferrera 2003, 2004; Fukushima et al. 2002; Xiao et al. 2007) and anticipatory pursuit, as lesioning of FEF results in its impairment (MacAvoy et al. 1991). Interconnected with FEF is the supplementary eye field (SEF) (Huerta and Kaas 1990; Schall et al. 1993), which is also thought to be heavily involved in generating anticipatory pursuit movements (de Hemptinne et al. 2008; Fukushima et al. 2004; Heinen et al. 1995; Heinen and Liu 1997). Given various representations of reference frames in SEF (Heinen and Liu 1997; Martinez-Trujillo et al. 2004; Olson and Gettner 1999; Russo and Bruce 1996; Tehovnik et al. 1998), the activities of SEF and FEF during both visually guided and anticipatory pursuit (Bruce and Goldberg 1985; de Hemptinne et al. 2008; Fukushima et al. 2002, 2004; Gottlieb et al. 1994; Heinen et al. 1995; Heinen and Liu 1997), their coding of head orientation signals (Fukushima et al. 2004; Fukushima et al. 2000; Gottlieb et al. 1993; Gottlieb et al. 1994; MacAvoy et al. 1991; Tanaka and Lisberger 2002a, 2002b), and close proximity in the pursuit circuitry (Maunsell and van Essen 1983), these findings lend credence to the idea that a separate pathway including SEF and FEF could be responsible for the coding of velocity memory and the transformation of anticipatory pursuit signals (Barnes and Collins 2008; de Hemptinne et al. 2008; Heinen and Liu 1997; Missal and Heinen 2004; Russo and Bruce 1996; Shichinohe et al. 2009; Stanton et al. 2005), while area MST could compute the velocity transformation for visually guided pursuit, as previously suggested (Blohm and Lefèvre 2010). Although we provide two hypotheses here, it remains to be seen what true neurophysiological mechanisms underlie the generation of anticipatory pursuit based on a retinal velocity memory that is updated for head roll changes.

Implications

If confirmed that velocity memories in the brain are retinal and thus spatially inaccurate, then this study has implications for any study using velocity memories for perception, motor planning, or decision-making (e.g., motion extrapolation, anticipatory pursuit, occluded pursuit, time-to-contact, etc.). This is because knowledge of the coordinate frame in which the neural representations in these tasks are coded could account for experimental findings and allow experimenters to make valuable behavioral and neurophysiological predictions. This study reveals that the neural transformation underlying the execution of memory-driven anticipatory pursuit movements can produce imperfect results compared with its online, visually guided counterpart. It remains to be seen if this difference in accuracy for movements based on memory and those based on current sensory input can be extended to other forms of predictive movements.

ACKNOWLEDGMENTS

The authors thank the participants for participation and Dr. A.Z. Khan for helpful comments on the manuscript.

GRANTS

This work was supported by Natural Sciences and Engineering Research Council of Canada, Canada Foundation for Innovation, the Botterell Fund (Queen's University, Kingston, ON, Canada), and Ontario Research Fund (Canada).

DISCLOSURES

No conflicts of interest, financial or otherwise, are declared by the author(s).

AUTHOR CONTRIBUTIONS

Author contributions: T.S.M. and C.A.P.-B. performed experiments; T.S.M. and G.B. analyzed data; T.S.M. and G.B. interpreted results of experiments; T.S.M. prepared figures; T.S.M. drafted manuscript; T.S.M. and G.B. edited and revised manuscript; T.S.M. and G.B. approved final version of manuscript; G.B. conception and design of research.

REFERENCES

- Ackerley R, Barnes GR. Extraction of visual motion information for the control of eye and head movement during head-free pursuit. *Exp Brain Res* 210: 569–582, 2011.
- Badler JB, Heinen SJ. Anticipatory movement timing using prediction and external cues. *J Neurosci* 26: 4519–4525, 2006.
- Balliet R, Nakayama K. Egocentric orientation is influenced by trained voluntary cyclorotary eye movements. *Nature* 275: 214–216, 1978.
- Barborica A, Ferrera VP. Modification of saccades evoked by stimulation of frontal eye field during invisible target tracking. *J Neurosci* 24: 3260–3267, 2004.
- Barborica A, Ferrera VP. Estimating invisible target speed from neuronal activity in monkey frontal eye field. *Nat Neurosci* 6: 66–74, 2003.
- Barnes GR. Cognitive processes involved in smooth pursuit eye movements. *Brain Cogn* 68: 309–326, 2008.
- Barnes GR, Asselman PT. The mechanism of prediction in human smooth pursuit eye movements. *J Physiol* 439: 439–461, 1991.
- Barnes GR, Barnes DM, Chakraborti SR, Ackerley R, Barnes GR. Ocular pursuit responses to repeated, single-cycle sinusoids reveal behavior compatible with predictive pursuit. *J Neurophysiol* 84: 2340–2355, 2000.
- Barnes GR, Collins CJS. Evidence for a link between the extra-retinal component of random-onset pursuit and the anticipatory pursuit of predictable object motion. *J Neurophysiol* 100: 1135–1146, 2008.
- Barnes GR, Donelan SF. The remembered pursuit task: evidence for segregation of timing and velocity storage in predictive oculomotor control. *Exp Brain Res* 129: 57–67, 1999.

- Barnes G, Grealy M, Collins S.** Volitional control of anticipatory ocular smooth pursuit after viewing, but not pursuing, a moving target: evidence for a re-afferent velocity store. *Exp Brain Res* 116: 445–455, 1997.
- Becker W, Fuchs AF.** Prediction in the oculomotor system: smooth pursuit during transient disappearance of a visual target. *Exp Brain Res* 57: 562–575, 1985.
- Blohm G, Lefèvre P.** Visuomotor velocity transformations for smooth pursuit eye movements. *J Neurophysiol* 104: 2103–2115, 2010.
- Blohm G, Missal M, Lefèvre P.** Interaction between smooth anticipation and saccades during ocular orientation in darkness. *J Neurophysiol* 89: 1423–1433, 2003a.
- Blohm G, Missal M, Lefèvre P.** Smooth anticipatory eye movements alter the memorized position of flashed targets. *J Vis* 3: 761–770, 2003b.
- Blohm G, Missal M, Lefèvre P.** Direct evidence for a position input to the smooth pursuit system. *J Neurophysiol* 94: 712–721, 2005.
- Blohm G, Optican LM, Lefèvre P.** A model that integrates eye velocity commands to keep track of smooth eye displacements. *J Comput Neurosci* 21: 51–70, 2006.
- Bruce CJ, Goldberg ME.** Primate frontal eye fields. I. Single neurons discharging before saccades. *J Neurophysiol* 53: 603–635, 1985.
- Burns JK, Blohm G.** Multi-sensory weights depend on contextual noise in reference frame transformations. *Front Hum Neurosci* 4: 221, 2010.
- Burns JK, Nashed JY, Blohm G.** Head roll influences perceived hand position. *J Vis* 11: 1–9, 2011.
- Carl JR, Gellman RS.** Human smooth pursuit: stimulus-dependent responses. *J Neurophysiol* 57: 1446–1463, 1987.
- Cerminara NL, Apps R, Marple-Horvat D.** An internal model of a moving visual target in the lateral cerebellum. *J Physiol* 587: 429–442, 2009.
- Collins CJS, Barnes GR.** Scaling of smooth anticipatory eye velocity in response to sequences of discrete target movements in humans. *Exp Brain Res* 167: 404–413, 2005.
- Curthoys IS, Dai MJ, Halmagyi GM.** Human ocular torsional position before and after unilateral vestibular neurectomy. *Exp Brain Res* 85: 218–225, 1991.
- de Brouwer S, Missal M, Barnes G, Lefèvre P.** Quantitative analysis of catch-up saccades during sustained pursuit. *J Neurophysiol* 87: 1772–1780, 2002a.
- de Brouwer S, Missal M, Lefèvre P.** Role of retinal slip in the prediction of target motion during smooth and saccadic pursuit. *J Neurophysiol* 86: 550–558, 2001.
- de Brouwer S, Yuksel D, Blohm G, Missal M, Lefèvre P.** What triggers catch-up saccades during visual tracking? *J Neurophysiol* 87: 1646–1650, 2002b.
- de Hemptinne C, Lefèvre P, Missal M.** Neuronal bases of directional expectation and anticipatory pursuit. *J Neurosci* 28: 4298–4310, 2008.
- Diamond SG, Markham CH, Simpson NE, Curthoys IS.** Binocular counterrolling in humans during dynamic rotation. *Acta Otolaryngol (Stockh)* 87: 490–498, 1979.
- Dieterich M, Brandt T.** Ocular torsion and tilt of subjective visual vertical are sensitive brainstem signs. *Ann Neurol* 33: 292–299, 1993.
- Fiehler K, Rösler F, Henriques DYP.** Interaction between gaze and visual and proprioceptive position judgements. *Exp Brain Res* 203: 485–498, 2010.
- Fujiwara K, Akao T, Kurkin S, Fukushima K.** Activity of pursuit-related neurons in medial superior temporal area (MST) during static roll-tilt. *Cereb Cortex* 21: 155–165, 2011.
- Fukushima J, Akao T, Takeichi N, Kurkin S, Kaneko CRS, Fukushima K.** Pursuit-related neurons in the supplementary eye fields: discharge during pursuit and passive whole body rotation. *J Neurophysiol* 91: 2809–2825, 2004.
- Fukushima K, Sato T, Fukushima J, Shinmei Y, Kaneko CRS.** Activity of smooth pursuit-related neurons in the monkey periaruate cortex during pursuit and passive whole-body rotation. *J Neurophysiol* 83: 563–587, 2000.
- Fukushima K, Yamanobe T, Shinmei Y, Fukushima J.** Predictive responses of periaruate pursuit neurons to visual target motion. *Exp Brain Res* 145: 104–120, 2002.
- Gellman R, Carl J.** Motion processing for saccadic eye movements in humans. *Exp Brain Res* 84: 660–667, 1991.
- Goonetilleke SC, Mezey LE, Burgess AM, Curthoys IS.** On the relation between ocular torsion and visual perception of line orientation. *Vision Res* 48: 1488–1496, 2008.
- Gottlieb JP, Bruce CJ, MacAvoy MG.** Smooth eye movements elicited by microstimulation in the primate frontal eye field. *J Neurophysiol* 69: 786–799, 1993.
- Gottlieb JP, MacAvoy MG, Bruce CJ.** Neural responses related to smooth-pursuit eye movements and their correspondence with electrically elicited smooth eye movements in the primate frontal eye field. *J Neurophysiol* 72: 1634–1653, 1994.
- Hamasaki I, Hasebe S, Ohtsuki H.** Static ocular counterroll: video-based analysis after minimizing the false-torsion factors. *Jpn J Ophthalmol* 49: 497–504, 2005.
- Haustein W, Mittelstaedt H.** Evaluation of retinal orientation and gaze direction in the perception of the vertical. *Vision Res* 30: 255–262, 1990.
- Heinen SJ.** Single neuron activity in the dorsomedial frontal cortex during smooth pursuit eye movements. *Exp Brain Res* 104: 357–361, 1995.
- Heinen SJ, Badler JB, Ting W.** Timing and velocity randomization similarly affect anticipatory pursuit. *J Vis* 5: 493–503, 2005.
- Heinen SJ, Liu M.** Single-neuron activity in the dorsomedial frontal cortex during smooth-pursuit eye movements to predictable target motion. *Vis Neurosci* 14: 853–865, 1997.
- Henriques DYP, Klier EM, Smith MA, Lowy D, Crawford JD.** Gaze-centered remapping of remembered visual space in an open-loop pointing task. *J Neurosci* 18: 1583–1594, 1998.
- Huerta MF, Kaas JH.** Supplementary eye field as defined by intracortical microstimulation: connections in macaques. *J Comp Neurol* 293: 299–330, 1990.
- Ilg UJ.** The role of areas MT and MST in coding of visual motion underlying the execution of smooth pursuit. *Vision Res* 48: 2062–2069, 2008.
- Ilg UJ, Thier P.** The neural basis of smooth pursuit eye movements in the rhesus monkey brain. *Brain Cogn* 68: 229–240, 2008.
- Inaba N, Miura K, Kawano K.** Direction and speed tuning to visual motion in cortical areas MT and MSTd during smooth pursuit eye movements. *J Neurophysiol* 105: 1531–1545, 2011.
- Inaba N, Shinomoto S, Yamane S, Takemura A, Kawano K.** MST neurons code for visual motion in space independent of pursuit eye movements. *J Neurophysiol* 97: 3473–3483, 2007.
- Jarrett CB, Barnes G.** Volitional selection of direction in the generation of anticipatory ocular smooth pursuit in humans. *Neurosci Lett* 312: 25–28, 2001.
- Johnston K, Everling S.** Neurophysiology and neuroanatomy of reflexive and voluntary saccades in non-human primates. *Brain Cogn* 68: 271–283, 2008.
- Keller EL, Gandhi NJ, Weir PT.** Discharge of superior collicular neurons during saccades made to moving targets. *J Neurophysiol* 76: 3573–3577, 1996.
- Keller E, Johnsen SD.** Velocity prediction in corrective saccades during smooth-pursuit eye movements in monkey. *Exp Brain Res* 80: 525–531, 1990.
- Ketner RE, Mahamud S, Leung H, Sitkoff N, Houk JC, Peterson BW.** Prediction of complex two-dimensional trajectories by a cerebellar model of smooth pursuit eye movement. *J Neurophysiol* 77: 2115–2130, 1997.
- Knox PC.** Stimulus predictability and the gap effect on presaccadic smooth pursuit. *Neuroreport* 9: 809–812, 1998.
- Knox PC.** The effect of the gap paradigm on the latency of human smooth pursuit of eye movement. *Neuroreport* 7: 3027–3030, 1996.
- Kowler E.** Cognitive expectations, not habits, control anticipatory smooth oculomotor pursuit. *Vision Res* 29: 1049–1057, 1989.
- Krauzlis RJ.** Recasting the smooth pursuit eye movement system. *J Neurophysiol* 91: 591–603, 2004.
- Krauzlis RJ, Miles FA.** Release of fixation for pursuit and saccades in humans: evidence for shared inputs acting on different neural substrates. *J Neurophysiol* 76: 2822–2833, 1996.
- Kurkin S, Akao T, Shichinohe N, Fukushima J, Fukushima K.** Neuronal activity in medial superior temporal area (MST) during memory-based smooth pursuit eye movements in monkeys. *Exp Brain Res* 214: 293–301, 2011.
- Lisberger SG.** Visual guidance of smooth-pursuit eye movements: sensation, action, and what happens in between. *Neuron* 66: 477–491, 2010.
- MacAvoy MG, Gottlieb JP, Bruce CJ.** Smooth-pursuit eye movement representation in the primate frontal eye field. *Cereb Cortex* 1: 95–102, 1991.
- Martinez-Trujillo J, Medendorp WP, Wang H, Crawford JD.** Frames of reference for eye-head gaze commands in primate supplementary eye fields. *Neuron* 44: 1057–1066, 2004.
- Maunsell JH, van Essen DC.** The connections of the middle temporal visual area (MT) and their relationship to a cortical hierarchy in the macaque monkey. *J Neurosci* 3: 2563–2586, 1983.

- Medina JF, Lisberger SG.** Encoding and decoding of learned smooth-pursuit eye movements in the floccular complex of the monkey cerebellum. *J Neurophysiol* 102: 2039–2054, 2009.
- Medina JF, Lisberger SG.** Links from complex spikes to local plasticity and motor learning in the cerebellum of awake-behaving monkeys. *Nat Neurosci* 11: 1185–1192, 2008.
- Missal M, Heinen SJ.** Supplementary eye fields stimulation facilitates anticipatory pursuit. *J Neurophysiol* 92: 1257–1262, 2004.
- Moore ST, Haslwanter T, Curthoys IS, Smith ST.** A geometric basis for measurement of three-dimensional eye position using image processing. *Vision Res* 36: 445–459, 1996.
- Nakayama K, Balliet R.** Listing's law, eye position sense, and perception of the vertical. *Vision Res* 17: 453–457, 1977.
- Nuding U, Ono S, Mustari MJ, Büttner U, Glasauer S.** A theory of the dual pathways for smooth pursuit based on dynamic gain control. *J Neurophysiol* 99: 2798–2808, 2008.
- Olson CR, Gettner SN.** Macaque SEF neurons encode object-centered directions of eye movements regardless of the visual attributes of instructional cues. *J Neurophysiol* 81: 2340–2346, 1999.
- Orban de Xivry JJ, Bennett SJ, Lefèvre P, Barnes GR.** Evidence for synergy between saccades and smooth pursuit during transient target disappearance. *J Neurophysiol* 95: 418–427, 2006.
- Orban de Xivry JJ, Lefèvre P.** Saccades and pursuit: two outcomes of a single sensorimotor process. *J Physiol* 584: 11–23, 2007.
- Pavlou M, Wijnberg N, Faldon ME, Bronstein AM.** Effect of semicircular canal stimulation on the perception of the visual vertical. *J Neurophysiol* 90: 622–630, 2003.
- Poljac E, Lankheet MJM, van den Berg AV.** Perceptual compensation for eye torsion. *Vision Res* 45: 485–496, 2005.
- Rambold H, Churchland A, Selig Y, Jasmin L, Lisberger SG.** Partial ablations of the flocculus and ventral paraflocculus in monkeys cause linked deficits in smooth pursuit eye movements and adaptive modification of the VOR. *J Neurophysiol* 87: 912–924, 2002.
- Ron S, Vieuille T, Droulez J.** Target velocity based prediction in saccadic vector programming. *Vision Res* 29: 1103–1114, 1989a.
- Ron S, Vieuille T, Droulez J.** Use of target velocity in saccadic programming. *Brain Behav Evol* 33: 85–89, 1989b.
- Ronchetti E.** Robustness aspects of model choice. *Stat Sin* 7: 327–338, 1997.
- Rottach KG, Zivotofsky AZ, Das VE, Averbuch-Heller L, Discenna AO, Poonyathalang A, Leigh RJ.** Comparison of horizontal, vertical and diagonal smooth pursuit eye movements in normal human subjects. *Vision Res* 36: 2189–2195, 1996.
- Russo GS, Bruce CJ.** Neurons in the supplementary eye field of rhesus monkeys code visual targets and saccadic eye movements in an oculocentric coordinate system. *J Neurophysiol* 76: 825–848, 1996.
- Schall JD, Morel A, Kaas JH.** Topography of supplementary eye field afferents to frontal eye field in macaque. Implications for mapping between saccade coordinate systems. *Vis Neurosci* 10: 385–393, 1993.
- Schreiber K, Haslwanter T.** Improving calibration of 3-D video oculography systems. *IEEE Trans Biomed Eng* 51: 676–679, 2004.
- Shaikh AG, Meng H, Angelaki DE.** Multiple reference frames for motion in the primate cerebellum. *J Neurosci* 24: 4491–4497, 2004.
- Shichinohe N, Akao T, Kurkin S, Fukushima J, Kaneko CRS, Fukushima K.** Memory and decision making in the frontal cortex during visual motion processing for smooth pursuit eye movements. *Neuron* 62: 717–732, 2009.
- Stanton GB, Friedman HR, Dias EC, Bruce CJ.** Cortical afferents to the smooth-pursuit region of the macaque monkey's frontal eye field. *Exp Brain Res* 165: 179–192, 2005.
- Suh M, Leung H, Kettner RE.** Cerebellar flocculus and ventral paraflocculus Purkinje cell activity during predictive and visually driven pursuit in monkey. *J Neurophysiol* 84: 1835–1850, 2000.
- Suh M, Leung H, Kettner RE.** Kinematic model relating complex 2D smooth pursuit eye movements and Purkinje cell firing rate in cerebellar flocculus and paraflocculus of the rhesus monkey. In: *Proceedings of the 9th Annual International Conference of the IEEE Engineering in Medicine and Biology Society*. Chicago, IL: IEEE Engineering in Medicine and Biology Society, 1997.
- Tanaka M, Lisberger SG.** Regulation of the gain of visually guided smooth-pursuit eye movements by frontal cortex. *Nature* 409: 191–194, 2001.
- Tanaka M, Lisberger SG.** Enhancement of multiple components of pursuit eye movement by microstimulation in the arcuate frontal pursuit area in monkeys. *J Neurophysiol* 87: 802–818, 2002a.
- Tanaka M, Lisberger SG.** Role of arcuate frontal cortex of monkeys in smooth pursuit eye movements. I. Basic response properties to retinal image motion and position. *J Neurophysiol* 87: 2684–2699, 2002b.
- Tehovnik EJ, Slocum WM, Tolias AS, Schiller PH.** Saccades induced electrically from the dorsomedial frontal cortex: evidence for a head-centered representation. *Brain Res* 795: 287–291, 1998.
- Thier P, Erickson RG.** Responses of visual-tracking neurons from cortical area MST-I to visual, eye and head motion. *Eur J Neurosci* 4: 539–553, 1992.
- Wade SW, Curthoys IS.** The effect of ocular torsional position on perception of the roll-tilt of visual stimuli. *Vision Res* 37: 1071–1078, 1997.
- Wells SG, Barnes GR.** Fast, anticipatory smooth-pursuit eye movements appear to depend on a short-term store. *Exp Brain Res* 120: 129–133, 1998.
- Xiao Q, Barboric A, Ferrera VP.** Modulation of visual responses in macaque frontal eye field during covert tracking of invisible targets. *Cereb Cortex* 17: 918–928, 2007.
- Yakusheva TA, Shaikh AG, Green AM, Blazquez PM, Dickman JD, Angelaki DE.** Purkinje cells in posterior cerebellar vermis encode motion in an inertial reference frame. *Neuron* 54: 973–985, 2007.
- Zink R, Bucher SF, Weiss A, Brandt T, Dieterich M.** Effects of galvanic vestibular stimulation on otolithic and semicircular canal eye movements and perceived vertical. *Electroencephalogr Clin Neurophysiol* 107: 200–205, 1998.